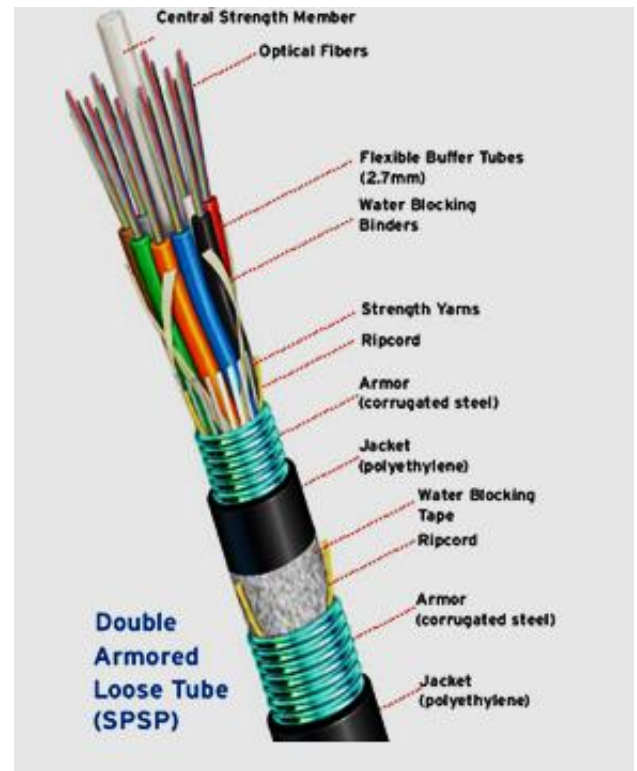
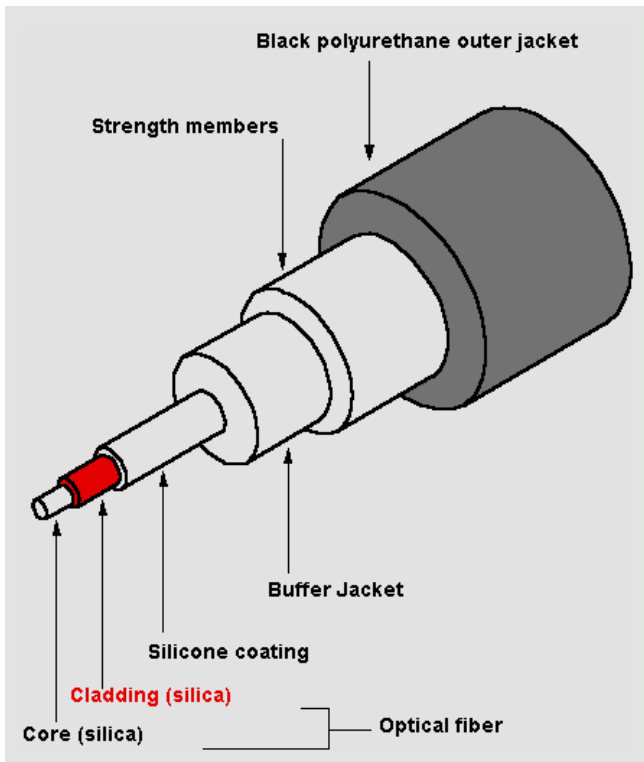
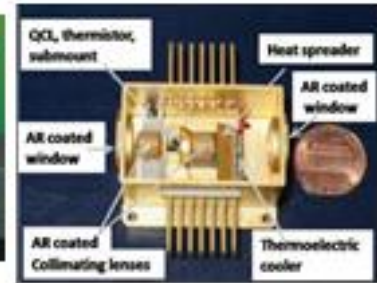
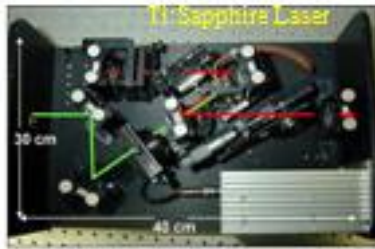


### Diary Page of Gordon Gould

The 28 years (1959 to 1987) patent war that it took for Gould to win the rights to his inventions became known as one of the most important patent battles in history. In the end, Gould was issued **forty-eight patents**, with the optical pumping, collisional pumping, and applications patents being the most important. **Between them, these technologies covered most lasers used at the time. For example, the first operating laser, a ruby laser, was optically pumped; the helium-neon laser is pumped by gas discharge.**

The delay—and the subsequent spread of lasers into many areas of technology—meant that the patents were much more valuable than if Gould had won initially. **Even though Gould had signed away eighty percent of the proceeds in order to finance his court costs, he made several million dollars.**

# Different Laser Systems



## Why is the bandwidth of optical fiber high?

Fiber-optic bandwidth is high both because of the speed with which data can be transmitted and the distance that data can travel without attenuation.

Optical fiber transmits data as pulses of light through glass wire, allowing data to travel at nearly the speed of light.

Fiber-optic cable has a wide range of frequencies over which data can travel that offers little loss or attenuation over distance.

## What determines the bandwidth of optical fiber versus copper wire?

The word bandwidth has two definitions, and they're closely related.

In computing and digital electronics, bandwidth means how much information can be transported over a channel per unit time, usually measured in bits per second.

In analog electronics, a band is a range of frequencies, and the bandwidth is the highest frequency minus the lowest frequency in the band, usually measured in Hertz. For example, the band of frequencies from 100 Hz to 130 Hz has a bandwidth of 30 Hz.

Now, when you send information down a copper cable, the frequencies that travel well (*not too much loss*) go from DC (0 frequency) to maybe 1 GHz. That's a bandwidth of 1 GHz.

When you send information down a fiber-optic, the frequencies that travel well (*not too much loss*) go from maybe 175 THz to 250 THz. That's a bandwidth of 75 THz = 75,000 GHz.

Thus a fiber can carry about 75,000 times more information than a copper cable.

The bandwidth differences are, effectively, the difference between photons and electrons. Copper uses electrons for data transmission, while fiber uses photons. Light is faster than electrical pulses, so fiber can transmit more bits of data per second



**Narinder Singh Kapany, the 'father of fiber optics' and the Indian Physicist who bent light.**

Narinder Singh Kapany was a pioneering scientist, entrepreneur, and philanthropist who served as a Regents Professor at UC Santa Cruz and a trustee of the UC Santa Cruz Foundation.

Kapany introduced the term "Fiber Optics" in a 1960 article in *Scientific American*, wrote the first book about the new field, and played a prominent role in advancing the field both as a researcher and as the founder of several optical technology companies.

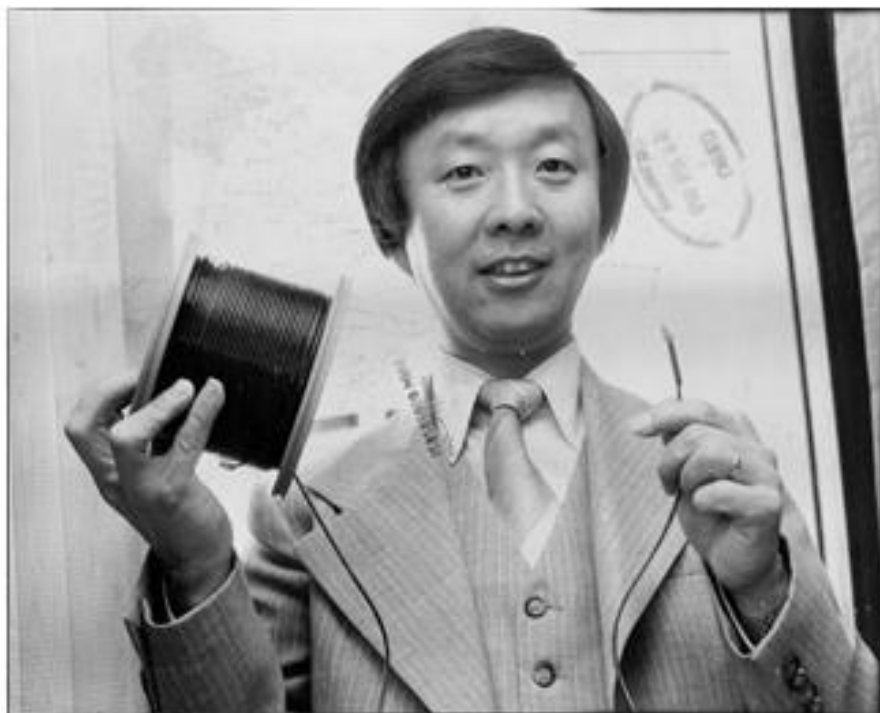
*As a graduate student working alongside Harold Hopkins at Imperial College in 1953, Kapany was the first to successfully transmit high-quality images through a bundle of optical fibers.*



*A fibre made of silicate or phosphate glass is doped to make the active gain medium. Some common doping elements in their increasing order of emitted wavelengths are:*

**Neodymium** ( $\text{Nd}^{3+}$ , 780-1100nm)  
Ytterbium ( $\text{Yb}^{3+}$ , 1000-1100nm)  
Praseodymium ( $\text{Pr}^{3+}$ , 1300nm)  
Erbium ( $\text{Er}^{3+}$ , 1460-1640nm)  
Thulium ( $\text{Tm}^{3+}$ , 1900-250nm)  
Holmium ( $\text{Ho}^{3+}$ , 2025-2200nm)  
&  
Dysprosium ( $\text{Dy}^{3+}$ , 2600-3400nm).

**Elias Snitzer, the pioneer of the Fiber Laser & Fiber Amplifier (1961).**



**Sir Charles Kuen Kao, pioneered the development and use of fiber optics in telecommunications. Kao was awarded the 2009 Nobel Prize in Physics**

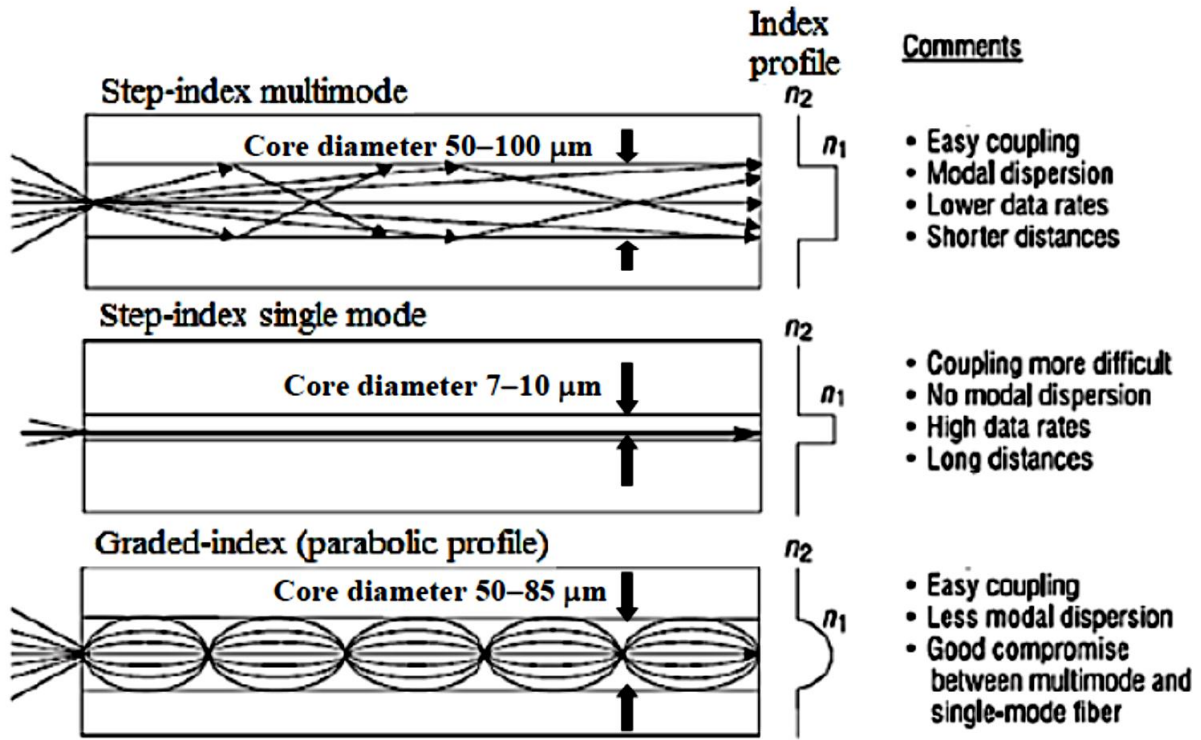


Fig. 1 Three basic types of fiber optic cables used in communication systems<sup>1</sup>.

### Numerical Aperture:

$$n_A \sin \theta_M = n_1 \cos \theta_c = (n_1^2 - n_2^2)^{1/2} = n_1 (2\Delta)^{1/2}$$

$$\text{Where, } \Delta = (n_1^2 - n_2^2) / 2n_1^2 = (n_1 - n_2)(n_1 + n_2) / 2n_1^2 \approx (n_1 - n_2) \cdot 2n_1 / 2n_1^2 \therefore \Delta \approx (n_1 - n_2) / n_1$$

### Refractive index characteristics of Graded Index Fiber:

The most popular form of r.i. profile is given by,

These two equations define graded index fiber.

$$\Rightarrow \begin{cases} n(r) = n_1 \left[ 1 - 2\Delta \left( \frac{r}{a} \right)^\alpha \right]^{1/2} & r < a \quad \text{--- (5)} \\ n(r) = n_1 (1 - 2\Delta)^{1/2} & r \geq a \quad \text{--- (6)} \end{cases}$$

$n_1$  = r.i. at the core axis.  
 $r$  = radial distance from the core axis.  
 $a$  = core radius  
 $n_2$  = r.i. of the cladding.  
 $\alpha$   $\Rightarrow$  defines the shape of the profile.

$\alpha$  can be varied to get different profiles. e.g if  $\alpha = 1$ , eq. (5) gives triangular profile; for  $\alpha = 2$  a parabolic and  $\alpha = \infty$  simplifies to a step index profile.

since  $r < a \quad (r/a)^\alpha \rightarrow 0 \therefore n(r) = n_1$  for  $r < a$   
 from definition  $n(r) = n_1 (1 - 2\Delta)^{1/2} = n_2$  for  $r \geq a$   
 so it is step index fibre.

In most commercial fibers, the ratio of core to cladding radius

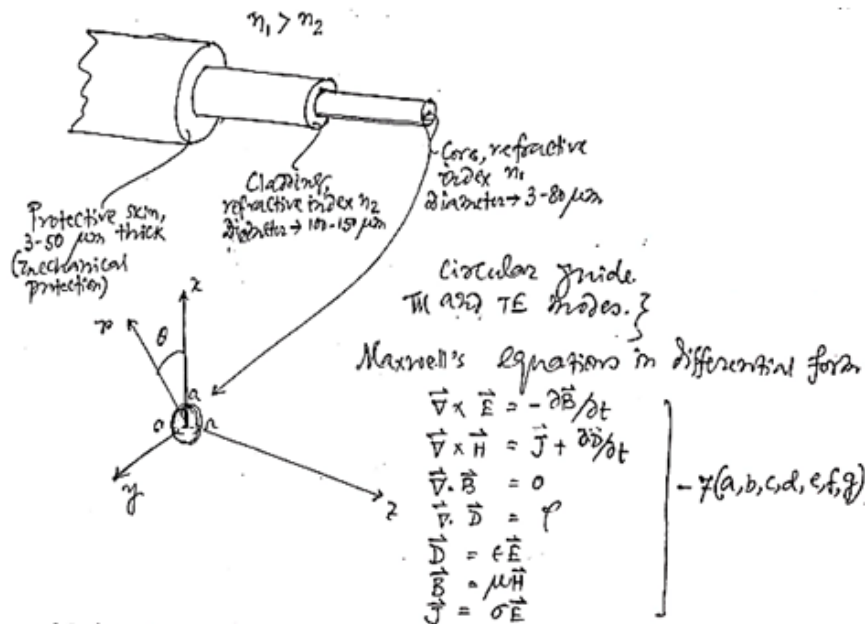
$$a_1/a_2 \sim 0.6$$

Thus for a 50  $\mu\text{m}$  thick core i.e. diameter 50  $\mu\text{m}$  and hence radius 25  $\mu\text{m}$  the cladding thickness is typically about 15  $\mu\text{m}$ . How?

$$a_1 = 25 \mu\text{m}$$

$$\therefore a_2 = 25/0.6 \mu\text{m} = 40 \mu\text{m} \text{ which is cladding radius.}$$

$$\therefore \text{Cladding thickness} = (40 - 25) \mu\text{m} = 15 \mu\text{m}$$



For propagation in z direction (since we are concerned with a structure that is expected to guide waves in z direction),

$$E_y(z,t) = E_0 e^{i(\omega t - \beta z)} \\
 H_y(z,t) = H_0 e^{i(\omega t - \beta z)}$$

Then,  $\frac{\partial E}{\partial z} = -i\beta E$  and  $\frac{\partial E}{\partial t} = i\omega E$   
 $\frac{\partial H}{\partial z} = -i\beta H$  and  $\frac{\partial H}{\partial t} = i\omega H$

We assume, conductivity  $\sigma = 0$ . Here  $\beta$  is known as propagation constant which is actually z component of  $\mathbf{k}$ .

We shall consider cylindrical coordinate system in which x, y and z are replaced by,  
 $x = r \cos \theta$  (r)       $y = r \sin \theta$  ( $\theta$ )       $z = z$  ( $\xi$ )

And the expression for  $\nabla \times \mathbf{A}$  in cylindrical coordinate is

$$\nabla \times \vec{A} = \begin{vmatrix} \vec{r}/r & \theta & \vec{z}/r \\ \frac{\partial}{\partial r} & \frac{\partial}{\partial \theta} & \frac{\partial}{\partial z} \\ A_r & rA_\theta & A_z \end{vmatrix}$$

Considering all these, we can express  $E_r$ ,  $E_\theta$ ,  $H_r$  and  $H_\theta$  in terms of  $E_z$  and  $H_z$  as:

$$\begin{aligned}
 E_r &= -\frac{i}{\gamma \epsilon^2} \left[ \gamma \beta \frac{\partial E_z}{\partial r} + \omega \mu_0 \frac{\partial H_z}{\partial \theta} \right] \\
 E_\theta &= -\frac{i}{\gamma \epsilon^2} \left[ \beta \frac{\partial E_z}{\partial \theta} - \gamma \omega \mu_0 \frac{\partial H_z}{\partial r} \right] \\
 H_r &= -\frac{i}{\gamma \epsilon^2} \left[ \gamma \beta \frac{\partial H_z}{\partial r} - \omega \epsilon \frac{\partial E_z}{\partial \theta} \right] \\
 H_\theta &= -\frac{i}{\gamma \epsilon^2} \left[ \beta \frac{\partial H_z}{\partial \theta} + \gamma \omega \epsilon \frac{\partial E_z}{\partial r} \right]
 \end{aligned}$$

Where,  $\xi^2 = k_1^2 - \beta^2$ ,  
 $k_1^2 = n_1^2 \omega^2 / c^2 = \omega^2 \mu_0 \epsilon_1$

The wave equations for  $E_z(r, \theta)$  and  $H_z(r, \theta)$  are modified in cylindrical coordinate as:

$$\frac{\partial^2 E_z}{\partial r^2} + \frac{1}{r} \frac{\partial E_z}{\partial r} + \frac{1}{r^2} \frac{\partial^2 E_z}{\partial \phi^2} + \xi^2 E_z = 0 \text{-----(5)}$$

$$\frac{\partial^2 H_z}{\partial r^2} + \frac{1}{r} \frac{\partial H_z}{\partial r} + \frac{1}{r^2} \frac{\partial^2 H_z}{\partial \phi^2} + \xi^2 H_z = 0 \text{-----(6)}$$

And these two wave equations are applicable in both the core and cladding.

Eqs. (5) and (6) are solved to obtain expressions for  $E_z$  and  $H_z$  in a round optical fiber. These expressions will then be substituted in Eqs.(1) to (4) to obtain a complete description of the fields in a fiber.

Let us try technique of separation of variables to obtain solution of Eq.(7). We assume,

$$E_z(t, r, \theta, z) = A g(r) h(\theta) e^{i(\omega t - \beta z)} \quad (7)$$

Since the **fiber has circular symmetry** we will choose a circular function as a trial solution for  $h(\theta)$  as

$$h(\theta) = e^{jv\theta}$$

Where  $v$  is a positive or negative integer.

Substituting all these,

$$\frac{\partial^2 E_z}{\partial r^2} + \frac{1}{r} \frac{\partial E_z}{\partial r} + \left( \xi^2 - \frac{v^2}{r^2} \right) E_z = 0$$

**Which is a Bessel's differential equation. Its solutions are Bessel function.**

The constraints we must place on  $g(r)$  are,

**$g(r)$  is finite for  $r < a$**

**&  $g(r) \rightarrow 0$  for  $r \gg a$**

Where  $a$  is the radius of the core. That means  $g(r)$  is finite inside core but zero outside.

Handwritten notes on a grey background:

Hence the forms of the solutions are,

$$E_z(r, \theta) = A J_v(\xi r) e^{jv\theta} \quad r < a$$

$$H_z(r, \theta) = B J_v(\xi r) e^{jv\theta} \quad r < a$$

for the fields in the core, and

$$E_z(r, \theta) = C K_v(\gamma r) e^{jv\theta} \quad r > a$$

$$H_z(r, \theta) = D K_v(\gamma r) e^{jv\theta} \quad r > a$$

in the cladding. The parameters  $\xi$  and  $\gamma$  are given by,

$$\xi^2 = k_1^2 - \beta^2 \quad \text{and} \quad \gamma^2 = \beta^2 - k_2^2$$

Where,  $k_1^2 = n_1^2 \omega^2 / c^2 = \omega^2 \mu_0 \epsilon_1$  and  $k_2^2 = n_2^2 \omega^2 / c^2 = \omega^2 \mu_0 \epsilon_2$

Here  $J_v(\xi r)$  is the Bessel function of the first kind and  $K_v(\gamma r)$  is the modified Bessel function of the second kind.

The roots of  $J_v(x) = 0$  are the zeros of the Bessel function which will be useful in determining which modes can propagate in the fiber.

The  $K_v(x)$  functions are +ve for all  $x$ . They are infinite for  $x=0$  and approach 0 as  $x$  increases i.e.

$$K_v(x) \rightarrow \infty \text{ for } x = 0$$

$$\text{\& } K_v(x) \rightarrow 0 \text{ as } x \rightarrow \infty$$



The boundary conditions for the fields at the core-cladding interface ( $r = a$ ) are:

$$E_{z1} = E_{z2}$$

$$E_{\phi 1} = E_{\phi 2}$$

$$H_{z1} = H_{z2}$$

$$H_{\phi 1} = H_{\phi 2}$$

Where subscripts 1 and 2 refer to the fields in the core and cladding respectively. Applying these conditions one can obtain the constants A, B, C and D.

In general there will be many different solutions, that is eigenvalues to the eigenvalue equation. Each eigenvalue defines a set of propagation parameters that represent one possible mode of propagation. Only modes that correspond to an eigenvalue can propagate in the fiber.

In general the permissible field configurations or modes that exist in a step index fiber have six field components. For the round fiber, hybrid modes exist as well as the TE and TM modes. The hybrid modes are denoted by  $HE_{\nu p}$  and  $EH_{\nu p}$  modes and have both longitudinal electric and magnetic field components present. Actually the hybrid modes correspond to propagating skew rays and the TE and TM modes to meridional rays. For special case  $\nu=0$ , only meridional rays propagate in the guide. i.e., special solution is

$\nu \neq 0$  six field components hybrid modes  
 $\nu = 0$  two characteristic eqns. only TE and TM modes.

An important parameter for each propagating mode is its cut-off frequency. A mode is cut-off when its field in the cladding ceases to be evanescent and is detached from the guide.

guide, that is, the field in the cladding does not decay. The rate of decay of the field in the cladding is determined by the value of the constant  $\gamma$ . For larger values of  $\gamma$ , it can be shown, the field is tightly concentrated inside and close to the core. With decreasing values of  $\gamma$ , the field reaches further out into the cladding. Finally for  $\gamma=0$  the field detaches itself from the guide. The frequency at which this happens is called the cut-off frequency. At cut-off,

$$\therefore \gamma = 0 = \sqrt{\beta^2 - \kappa_2^2}$$

$$\sim \beta^2 = \kappa_2^2 \quad \text{--- (26)}$$

where,  $\kappa_2^2 = \omega^2 \mu_0 \epsilon_2$  --- (27)

In the core of the guide at cutoff we have,

$$\alpha^2 = \kappa_1^2 - \beta^2 \quad \text{--- (21a)}$$

$$\text{where } \kappa_1^2 = \omega^2 \mu_0 \epsilon_1 \quad \text{--- (28)}$$

$\therefore$  we can obtain an expression for the cut-off frequency  $\omega_c$  of a mode by substituting eq. (26) into 21(a).

$$\alpha^2 = \kappa_1^2 - \kappa_2^2 = \omega_c^2 \mu_0 (\epsilon_1 - \epsilon_2) \quad \text{--- (29)}$$

$$\therefore \omega_c = \frac{\alpha}{\sqrt{\mu_0 (\epsilon_1 - \epsilon_2)}} \quad \text{--- (30)}$$

The cut off frequency of a mode can be zero if  $k_{z0} = 0$ . One and only one mode can exist in an optical fiber with  $\omega_c = 0$ . This mode is the hybrid  $HE_{11}$  mode which exists for all frequencies. It is therefore possible to design and operate a single-mode optical fiber. The single-mode fiber has a very small core diameter and small refractive index difference between the core and cladding.

To appreciate the significance of the cut-off parameter  $\beta_c$ , let us define it in terms of the physical parameters of the fiber from eq. 29,

As is evident, the condition  $\beta_c = 0$  or  $\omega_c = 0$  does not indicate that  $V$  is also zero. It can be shown that for  $V < 2.405$  one mode can occur, which is  $HE_{11}$ .

$$\beta_c a = \omega_c \sqrt{\mu_0 \epsilon_0} (\sqrt{n_1^2 - n_2^2}) a \quad (31)$$

Since  $\omega_c/c = \beta_c$

$$\omega_c \sqrt{\mu_0 \epsilon_0} = \frac{2\pi}{\lambda_c} \quad (32)$$

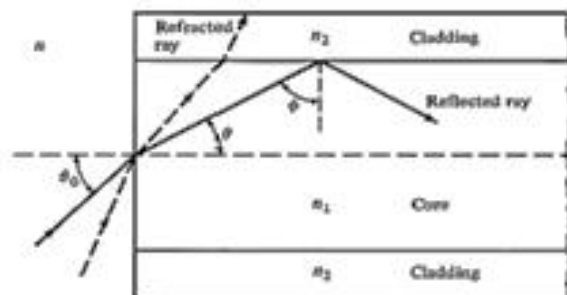
We obtain,

$$V \equiv \beta_c a = \frac{2\pi a}{\lambda_c} \sqrt{n_1^2 - n_2^2} \quad (33) \quad \text{Same as eq. 23}$$

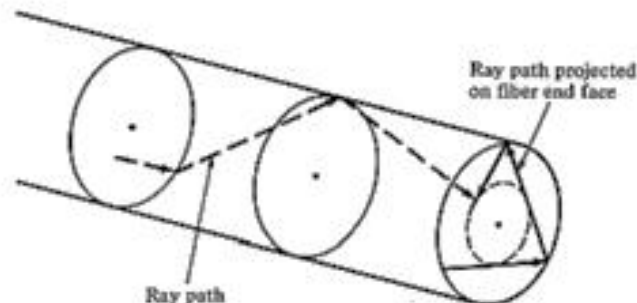
The cut-off parameter  $\beta_c a$  is usually called the "V" number of the fiber. The number of propagating modes in the step-index fiber is proportional to the its "V" number. The total number of modes that can exist in a step-index fiber for a given value of  $V$  is,  $N = 4V^2/\pi^2$

## Meridional and skew rays

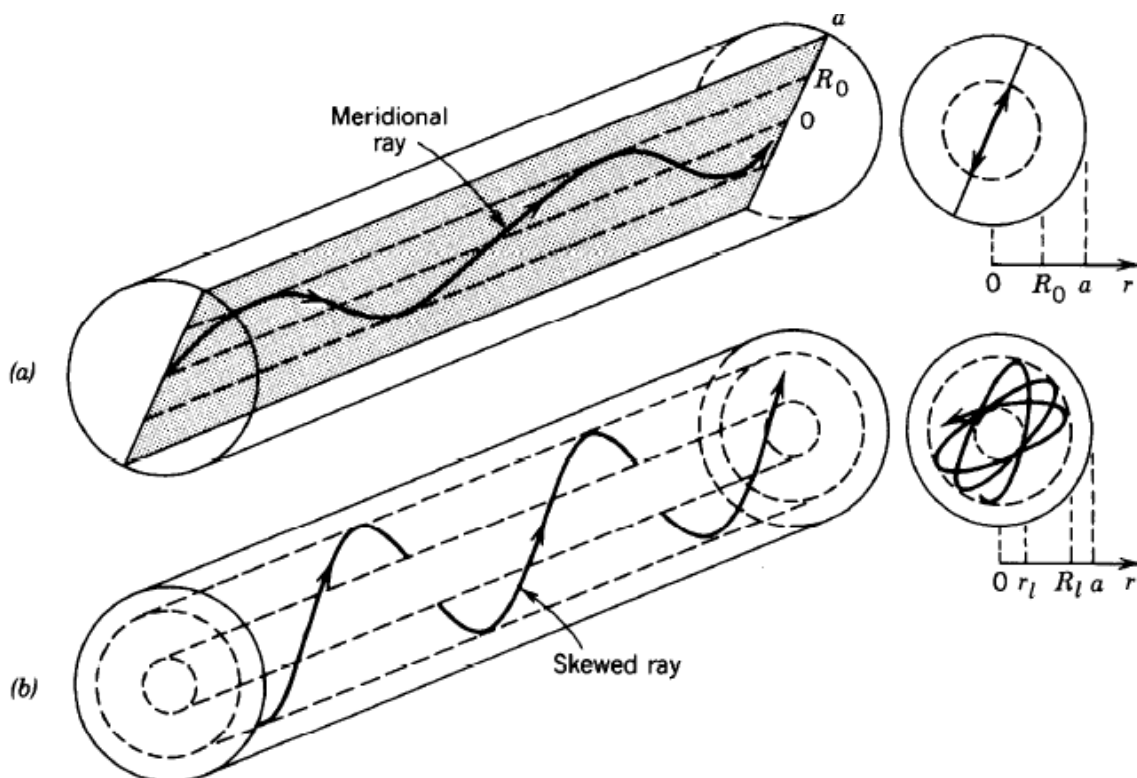
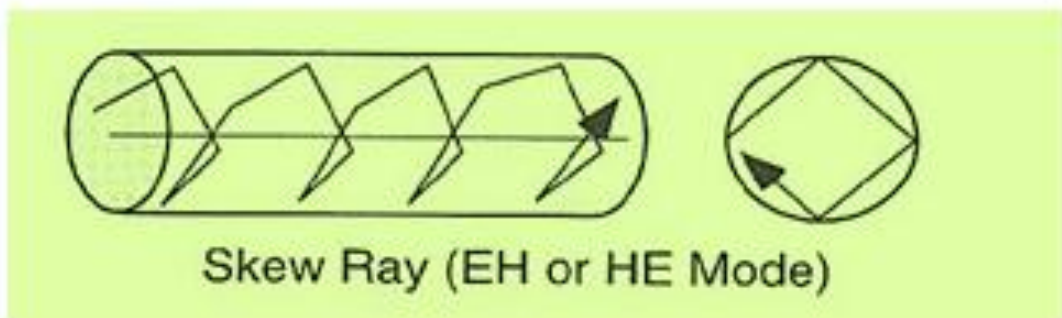
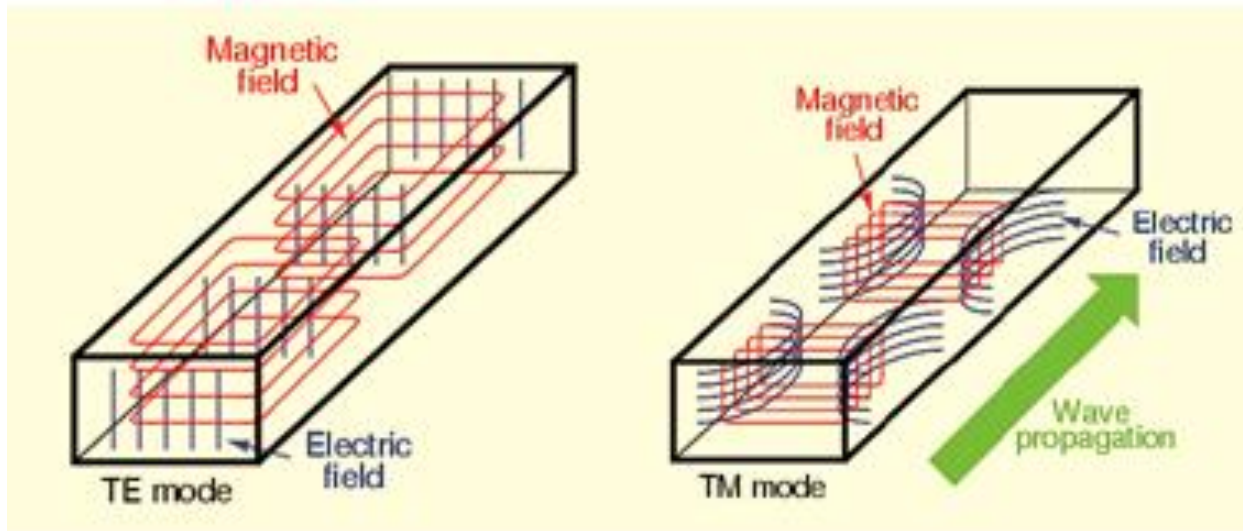
- A *meridional ray* is one that has no  $\phi$  component – it passes through the  $z$  axis, and is thus in direct analogy to a slab guide ray.
- Ray propagation in a fiber is complicated by the possibility of a path component in the  $\phi$  direction, from which arises a *skew ray*.
- Such a ray exhibits a spiral-like path down the core, never crossing the  $z$  axis.



Meridional ray

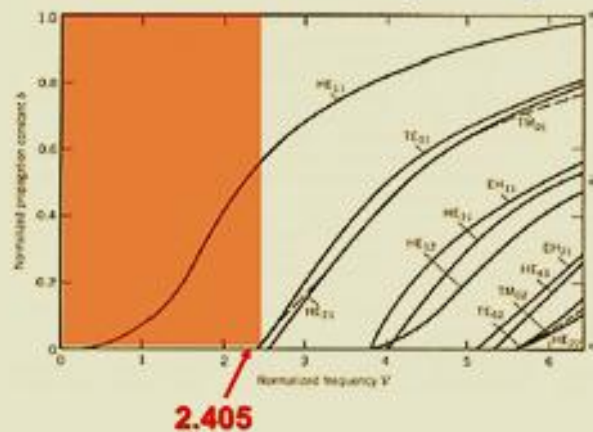


Skew ray



A skewed ray lies in a plane offset from the fiber axis by a distance  $R$ . The ray is identified by the angles  $\theta$  and  $\phi$ . It follows a helical trajectory confined within a cylindrical shell of radii  $R$  and  $a$ . The projection of the ray on the transverse plane is a regular polygon that is not necessarily closed.

## Normalized Propagation Constant as a Function of Normalized Frequency



A fiber becomes single-mode when its  $V$  number  $< 2.405$  (the first root of the  $J_0$  Bessel function).

In a single-mode fiber only the  $HE_{11}$  mode can propagate. This mode is often called the fundamental mode of the fiber, or  $LP_{01}$  mode (weakly guiding approximation).

## Signal distortion in optical waveguides

- **Dispersion** used to describe the process by which a signal propagating in a optical fibre is degraded because the various signal frequencies have different propagation velocities.
- Main causes of **intra-modal dispersion** or **chromatic dispersion**
  - Material dispersion
  - Waveguide dispersion
- Inter-modal dispersion (multimode fibres)

## Delay Distortion in a Single Mode Optical Fiber

The degradation of an optical pulse propagating through the fiber specifically occurs due to:

### Intra Modal or Chromatic dispersion:

1. Material dispersion ( $D_m$ )
2. Waveguide dispersion ( $D_w$ )

*The first part is the dispersion induced on the light by the material used in the waveguide and this is known as material dispersion. The second part is the impact of the actual waveguide structure, and it is known as waveguide dispersion.*

Dispersion  $D$  of a fiber is measured by,

$$D = (1/L) (d\tau_g/d\lambda) \text{ ps/km.nm}$$

*i.e. Picoseconds per nanometer of source bandwidth per kilometer of distance traversed.*

The speed of propagation of monochromatic light in an optical fiber is,

$$u_{\text{phase}} = c/n_1(\lambda)$$

which is the phase velocity of the light wave and it is different for different wavelength.

In transmitting a pulse of light through the fiber, the pulse can be expressed as the summation of a number of sine and cosine functions, which is known as the spectrum of the pulse. If the spectrum is centered on a frequency,  $\omega$ , and has a small spectral width around  $\omega$ , then a velocity can be associated with this group of frequencies, and this is known as the group velocity.

So corresponding to the group velocity, say  $v_g$ , a group index  $N_g$ , can be defined as corresponding to the group of frequencies around  $\omega$ . Therefore,

$$v_g = c/N_g$$

For pulse travelling  $L$  distance, Group delay  $\tau_g$  is defined as:

$$\begin{aligned}\tau_g &= L/v_g = L \cdot dk_1/d\omega = L \cdot d(n_1 \cdot \omega/c)/d\omega \\ &= (L/c) d(n_1 \cdot \omega)/d\omega = (L/c) [n_1 + \omega \cdot dn_1/d\omega] \\ &= L \cdot N_g/c\end{aligned}$$

$$\begin{aligned}\therefore N_g &= n_1 + \omega \cdot dn_1/d\omega \\ &= n_1 + \omega \cdot (dn_1/d\lambda) \cdot (d\lambda/d\omega) \\ &= n_1 + \omega \cdot (dn_1/d\lambda) \cdot (-\lambda/\omega) \quad [\text{as, } \lambda = 2\pi c/\omega] \\ &= n_1 - \lambda \cdot (dn_1/d\lambda)\end{aligned}$$

Hence the packet of frequencies corresponding to the pulse will arrive at the output of the fiber sometime after the pulse is launched. This delay is the group delay  $\tau_g$ .

If the energy propagates a distance  $L$  in the fiber, the spread in the arrival times of energy propagating at different wavelengths  $\lambda_1$  and  $\lambda_2$  is,

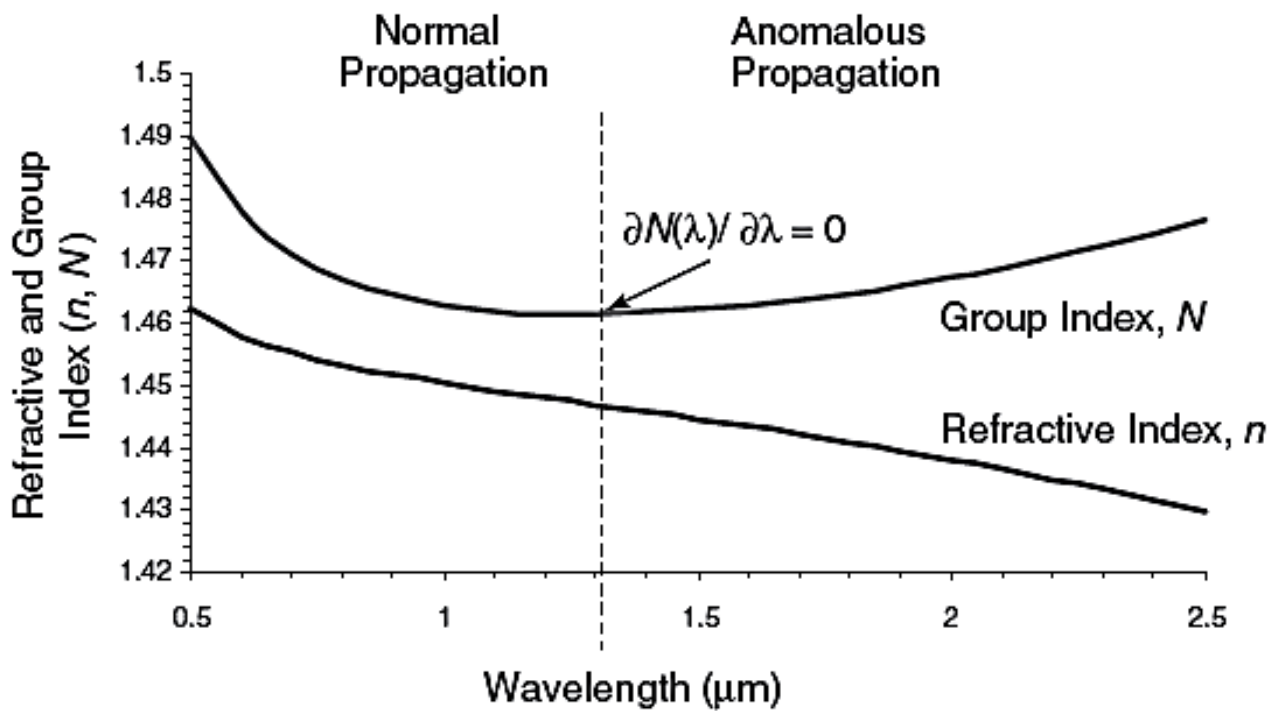
$$\begin{aligned}\Delta\tau_m &= [L \cdot N_g(\lambda_1) - L \cdot N_g(\lambda_2)](1/c) = - [L \cdot N_g(\lambda_2) - L \cdot N_g(\lambda_1)](1/c) \\ &= - (L/c) \cdot (dN_g/d\lambda) \cdot \Delta\lambda = - (L/c) \cdot [(dn/d\lambda) - \lambda(d^2n/d\lambda^2) - (dn/d\lambda)] \cdot \Delta\lambda \\ &= + (L/c) \cdot \lambda(d^2n/d\lambda^2) \cdot \Delta\lambda\end{aligned}$$

$$\therefore \Delta\tau_m = (L/c) \cdot [\lambda_0^2 (d^2n/d\lambda^2)] \cdot (\Delta\lambda/\lambda)$$

If  $\lambda_0 = 820 \text{ nm}$ ,  $\Delta\lambda = 1 \text{ nm}$  i.e.  $\Delta\lambda/\lambda = 0.12\%$

It can be shown that pulse broadening in 1Km fiber due to these chromatic dispersion  $\sim 100 \text{ ps}$ .

**Condition for Zero dispersion is,  $\lambda_0^2 (d^2n/d\lambda^2) = \lambda_0 (dN_g/d\lambda) = 0$**



$\lambda_0$ (nm)	$D_\lambda$ (ps/Km.nm)
820	-80
1.32	0
1.55	+17

**For any material, the zero dispersion is the wavelength at which the curve of the refractive index has an inflection point ( $\lambda_0$  point).**

➤ For  $\lambda < \lambda_0$ ,  $N_g$  decreases as  $\lambda$  decreases.

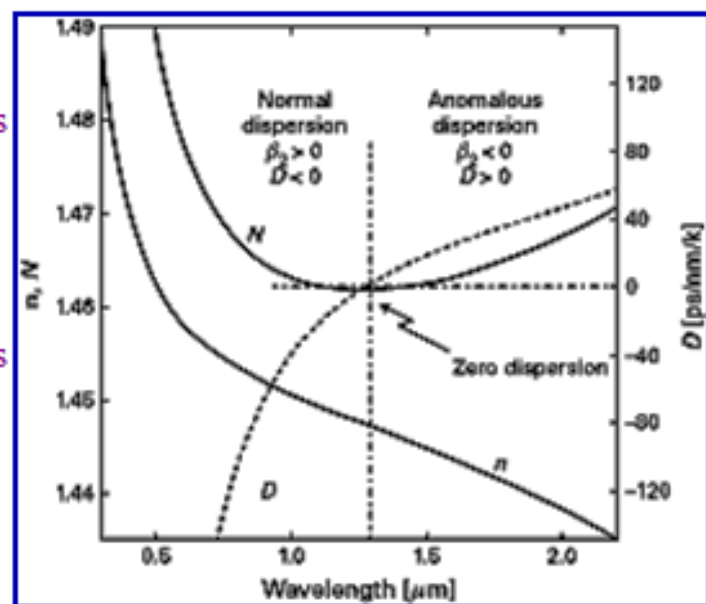
$$\therefore V_\lambda(\text{IR}) > V_\lambda(\text{UV})$$

**Normal group dispersion**

➤ For  $\lambda > \lambda_0$ ,  $N_g$  increases as  $\lambda$  increases.

$$\therefore V_\lambda(\text{IR}) < V_\lambda(\text{UV})$$

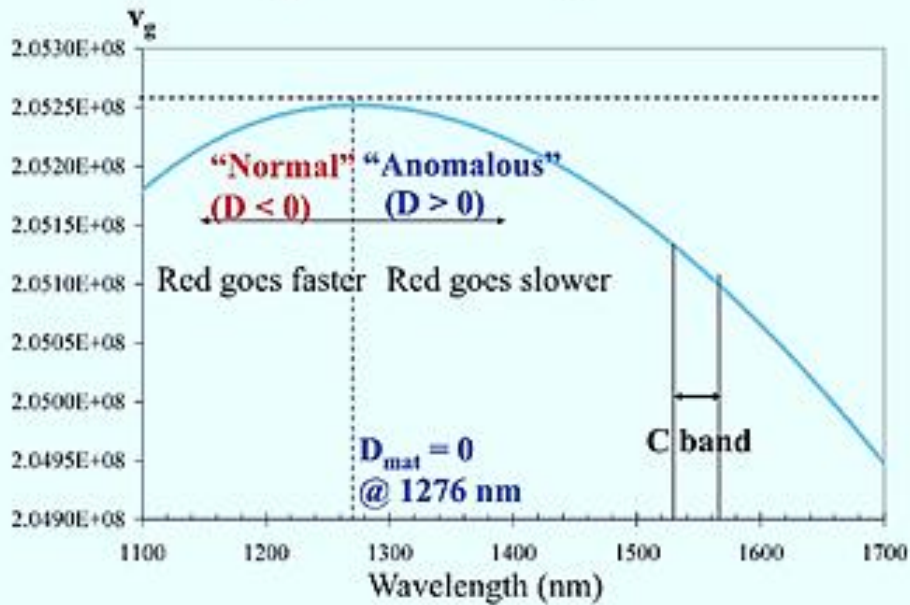
**Anomalous group dispersion**



**Material dispersion of pure silica.**

# Material Dispersion

Variation of  $V_g$  with wavelength for fused silica



Material dispersion  $D_{mat} = 0$  at  $\lambda \sim 1276$  nm for fused silica. This  $\lambda$  is referred to as the **zero-dispersion wavelength  $\lambda_{ZD}$** .

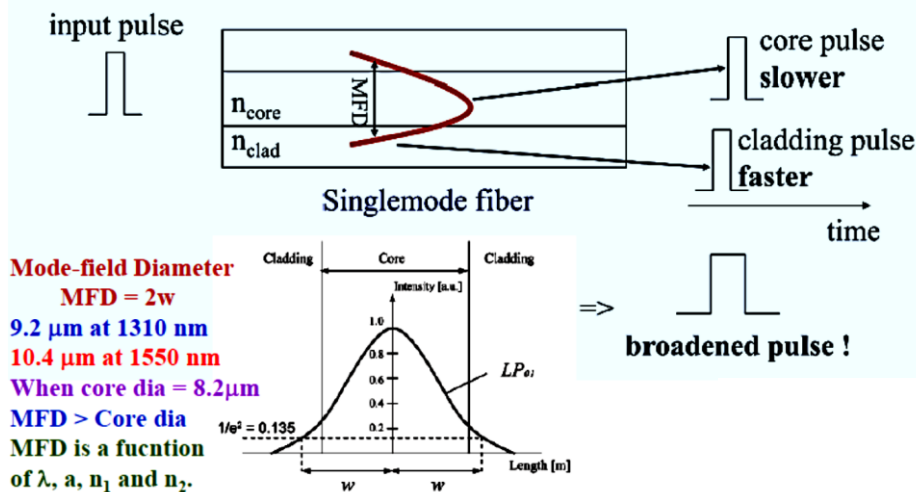
*Please note that this in this figure  $v_g$  is plotted against  $\lambda$ .*

In single mode fiber, about 20% energy travels in the cladding. This signal will have a different velocity than the signal travels in the core because  $n_2 < n_1$ . This phenomena pave way to waveguide dispersion. This dispersion will be dominant in single mode fibers and not significant in multimode fibers.

**Waveguide dispersion** depends upon the fiber design. The propagation constant is a function of the ratio of fiber dimension (i.e. core radius) to the wavelength or  $a/\lambda$ .

# Waveguide Dispersion

Waveguide dispersion is chromatic dispersion which arises from waveguide effects: the dispersive phase shifts for a wave in a waveguide differ from those which the wave would experience in a homogeneous medium.

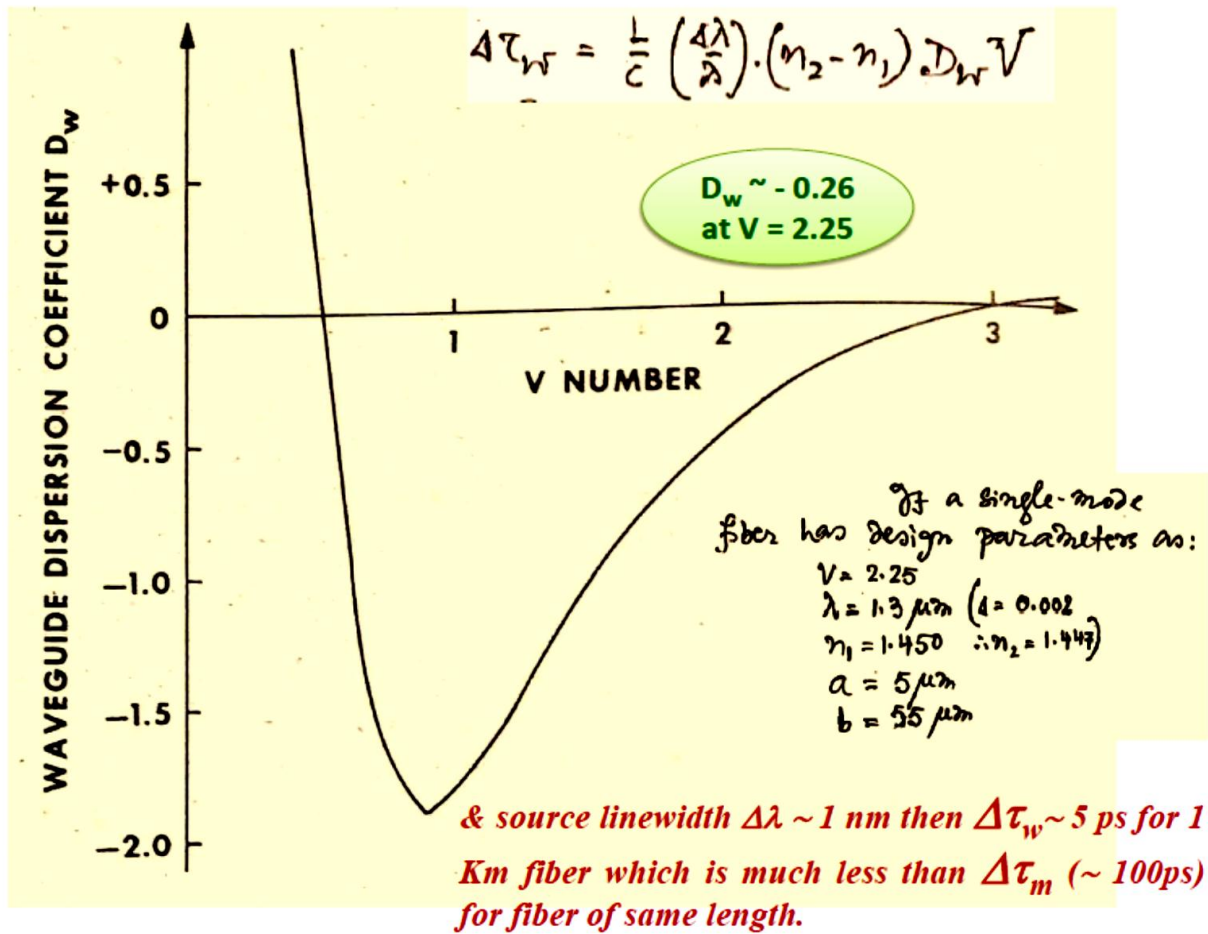


1. The waveguide dispersion is *usually negative* for a given single-mode fiber. The magnitude increases with increase in wavelength. It is usually caused by the difference of refractive index of refraction between core and cladding, resulting in a “drag” effect between the core and cladding portions of the power.
2. If the core radius  $a$  (of a single-mode fiber) is made smaller and the value of  $\Delta$  is made larger, the magnitude of the waveguide dispersion increases. *Thus we can tailor the waveguide dispersion by changing the refractive index profile.*
3. Waveguide dispersion is significant only in fibers carrying 5 to 10 modes. *Since multimode optical fibers carry hundreds of modes, they will not have observable waveguide dispersion.*

It can be shown that,

$$\Delta\tau_w = \frac{L}{c} \left( \frac{\Delta\lambda}{\lambda} \right) \cdot (n_2 - n_1) D_w V$$

Where  $D_w$  is a dimensionless dispersion coefficient which is a function of  $V$  number of the fiber.



### Delay Distortion in a Step Index Multimode Optical Fiber:

What we are concerned with is Inter-Modal dispersion which is caused by the different group delays of the modes. Since now many modes are present so instead of propagation constant  $k$  we will use  $\beta$  which is component of  $k$  in propagation direction ( $z$ ). We know that,

$$\beta = [k_1^2 - \xi^2]^{1/2} = [n_1^2 k_0^2 - \xi^2]^{1/2} \quad \text{where } k_0 = 2\pi/\lambda_0 \text{ and } k_1 = n_1 k_0$$

Hence Group delay for propagation of distance  $L$  in fiber is,

$$\therefore \tau_g = L \cdot d\beta/d\omega = L \cdot (d\beta/dk_0) \cdot (dk_0/d\omega) = (L/c) \cdot (d\beta/dk_0)$$

$$\text{Again, } V = a \cdot k_0 (n_1^2 - n_2^2)^{1/2}$$

$$\therefore dV/dk_0 = a \cdot (n_1^2 - n_2^2)^{1/2} = V/k_0$$

$$\therefore \tau_g = (L/c) \cdot (d\beta/dk_0) = (L/c) \cdot (d\beta/dV) \cdot (dV/dk_0) = (L/c) \cdot (V/k_0) \cdot (d\beta/dV)$$



A normalised propagation constant is defined as,

$$b = (\gamma a)^2 / V^2 \text{ where } \gamma = [\beta^2 - k_2^2]^{1/2}$$

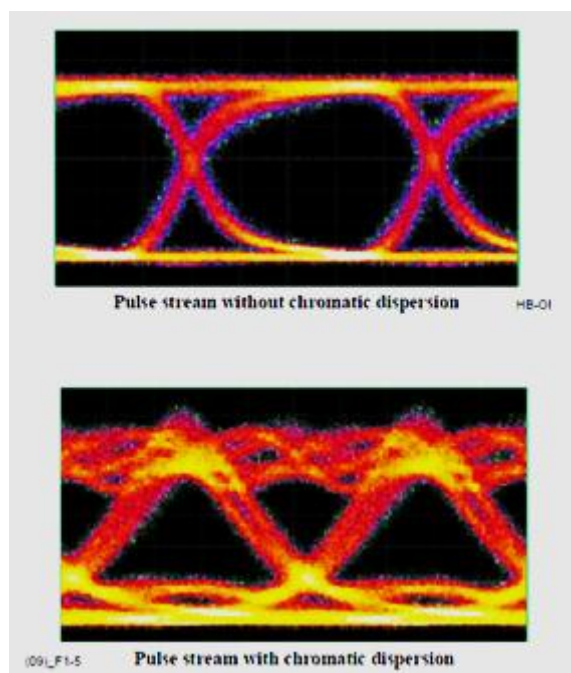
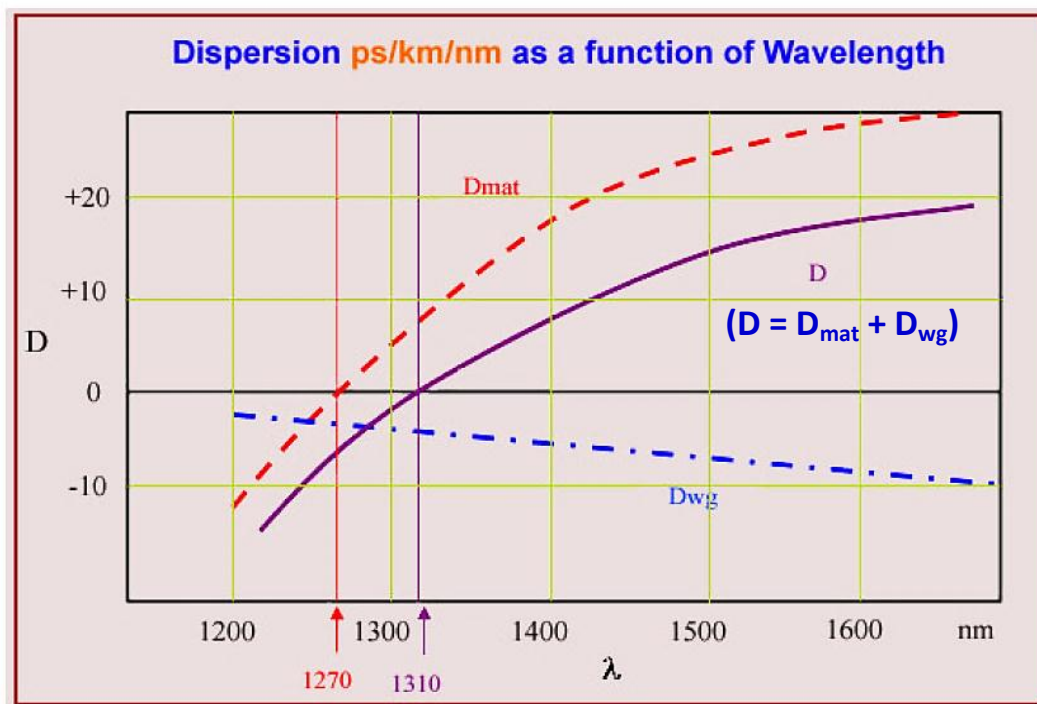
For weakly guiding fibers  $\Delta \approx (n_1 - n_2) / n_1 \ll 1$ .

Hence,  $V \sim a \cdot k_0 \cdot n_2 \cdot (2\Delta)^{1/2}$  **And**  $\gamma \sim V \sqrt{b/a} = k_0 \cdot n_2 \cdot (2b\Delta)^{1/2}$

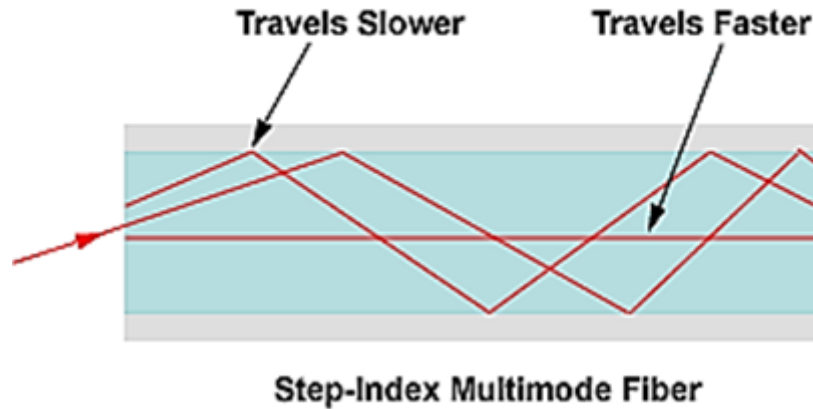
$$\therefore \beta = [n_2^2 k_0^2 + \gamma^2]^{1/2} = [n_2^2 k_0^2 (1 + 2b\Delta)]^{1/2} \sim n_2 k_0 (1 + b\Delta)$$

$$\begin{aligned} \therefore \tau_g &= (L/c) \cdot (d\beta/dk_0) = (L/c) \cdot [d\{n_2 k_0 (1 + b\Delta)\}/dk_0] \\ &= (L/c) \cdot d(n_2 k_0)/dk_0 + (L/c) \cdot [d(n_2 k_0 b\Delta)/dV] \cdot [dV/dk_0] \\ &= (L/c) \cdot d(n_2 k_0)/dk_0 + (L/c) \cdot [d(n_2 k_0 b\Delta)/dV] \cdot [V/k_0] \\ &= \tau_m + \tau_w \\ &= \text{Material dispersion} + \text{Waveguide delay} \end{aligned}$$

However, it must be noted that depending on transmission wavelength the sign of material dispersion and waveguide dispersion can have opposite sign.



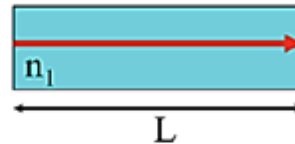
## Modal Dispersion



**Estimate modal dispersion pulse broadening using phase velocity**

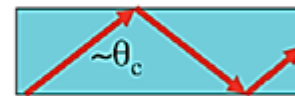
□ A zero-order mode traveling near the waveguide axis needs time:

$$t_0 = L/v_{m=0} \approx Ln_1/c \quad (v_{m=0} \approx c/n_1)$$



□ The highest-order mode traveling near the critical angle needs time:

$$t_m = L/v_m \approx Ln_2/c \quad (v_m \approx c/n_2)$$



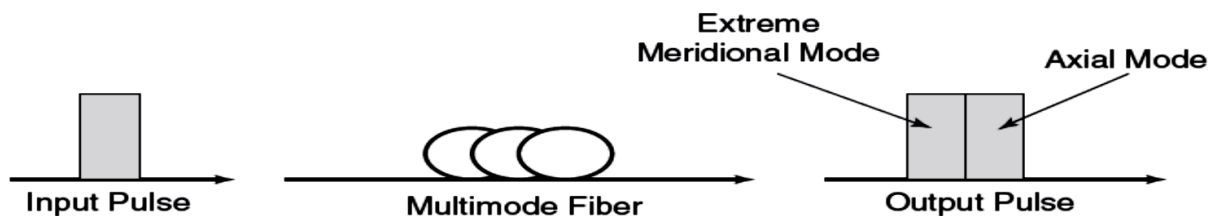
=> The pulse broadening due to modal dispersion:

$$\begin{aligned} \Delta T &\approx t_0 - t_m \approx (L/c)(n_1 - n_2) = L/c \Delta n_1 \text{ for } \Delta \ll 1 \\ &\approx (L/2cn_1) NA^2 \quad (n_1 \sim n_2) \quad (1) \end{aligned}$$

It can be shown that, the r.m.s broadening of the pulse is:

$$\sigma_s|_{\text{step}} = \frac{1}{2\sqrt{3}} \cdot \Delta \cdot \frac{Ln_1}{c} = \frac{1}{2\sqrt{3}} \cdot (NA)^2 \cdot \frac{L}{2cn_1} \quad (2)$$

To appreciate the impact of this differential delay, let us assume that a pulse of nominal width  $T$  is launched into the fiber. *If the differential delay is equal to the pulse width*, the output consists of two pulses occupying a total width of  $2T$  as shown.



The receiver will therefore detect two pulses when only one was sent. This effect is called the intermodal dispersion of the fiber, and it is an additional dispersion imparted on the pulse.

To appreciate the quantities involved, consider a multimode step index fiber of 10 km length with a core refractive index of 1.5 and  $\Delta = 2\%$ . Then from equation (2) the r.m.s. pulse broadening is,

$$\sigma_s|_{\text{step}} = \frac{1}{2\sqrt{3}} \cdot \Delta \cdot \frac{Ln_1}{c} = \frac{1}{2\sqrt{3}} \cdot 0.02 \cdot \frac{10 \times 10^3 \times 1.5}{2.998 \times 10^8} = 2.88 \times 10^{-2} \frac{ns}{m} \times 10 \times 10^3 m = 288 \text{ ns.} \quad (3)$$

The maximum transmission bitrate in terms of the pulse r.m.s. width is given by,

$$B_{T \max} = \frac{0.25}{\sigma_{\text{pulse}}} \quad (4)$$

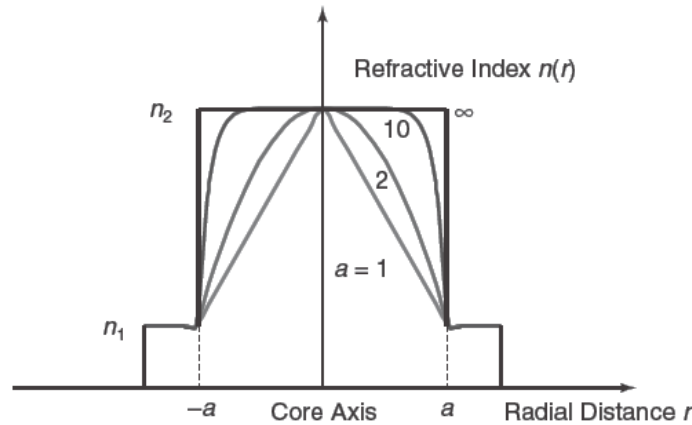
Therefore, for  $\sigma_s = \sigma = 288$  ns, the maximum bitrate is 868 Kbit/s, which is not a useful value for most modern applications.

The key question now is whether the differential delay for a multimode fiber can be improved. The reason the differential delay between the axial mode and the extreme meridional mode is high is that **the meridional mode has to reach the boundary between core and cladding before it is reflected back into the core**. If the flight time of a meridional mode is reduced, then the differential delay will also be reduced. This can be achieved with the use of graded index fiber.

The general equation for the variation of refractive index with radial distance is,

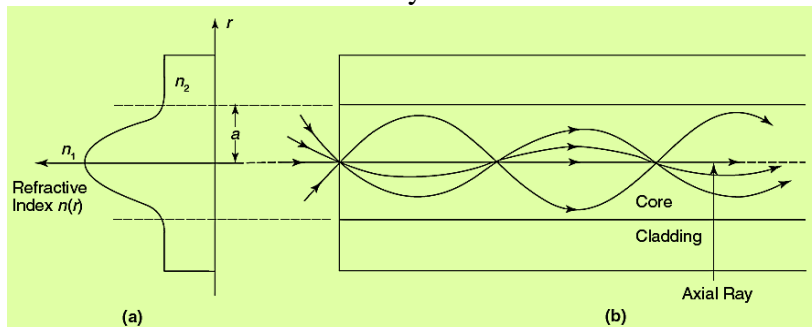
$$n(r) = \begin{cases} n_1(1 - 2\Delta(r/a)^\alpha)^{1/2} & r < a \text{ core} \\ n_1(1 - 2\Delta)^{1/2} = n_2 & r \geq a \text{ cladding} \end{cases}$$

where  $\Delta$  is the relative refractive index difference,  $r$  is the axial distance, and  $a$  is the profile parameter that gives the refractive index profile. Figure below illustrates the fiber refractive index for various values of the profile parameter  $a$ . The step index profile is obtained by setting  $a = \infty$ .



**Fiber refractive index for different values of the profile parameter  $a$ .**

The improvement in differential delay can be observed by considering the modes of a multimode fiber with the profile parameter  $a$  set to 2. Two effects may be observed. First, the axial mode propagates through the section of the fiber core where the refractive index has its maximum value, which implies that the axial mode is slowed down. The meridional modes are bent toward the axis of the fiber, reducing their flight time. Together these two effects reduce the differential delay.



If electromagnetic theory is employed to analyze the differential delay, the value obtained is,

$$\Delta\tau_s|_{\text{graded}} = \frac{\Delta^2}{8} \frac{Ln1}{c} = \Delta\tau_s|_{\text{step}} \times \frac{\Delta}{8} \quad (6)$$

The implication of this equation is to highlight the fact that the reduction of the differential delay for step index fiber is  $\Delta/8$ . The r.m.s. pulse broadening is now given by,

$$\sigma_s|_{\text{index}} = \frac{1}{2\sqrt{3}} \Delta \frac{Ln1}{c} \times \frac{\Delta}{10} = \sigma_s|_{\text{step}} \times \frac{\Delta}{10} \quad (7)$$

and there is a  $\Delta/10$  reduction in the r.m.s. pulse broadening. It is now straightforward to compare the r.m.s. pulse broadening for step and graded index fibers. From the example studied before, we have a 10 km graded index fiber with a core refractive index of 1.5 and  $\Delta = 2\%$ .

$$\sigma_{s|_{\text{index}}} = \sigma_{s|_{\text{step}}} \times \frac{\Delta}{10} = 288 \text{ ns} \times \frac{0.02}{10} = 0.576 \text{ ns}$$

and the maximum bitrate that can be used with this graded index fiber is now 434 Mbit/s!

Comparing the r.m.s. pulse broadening of the two fibers for a length of 1 km, one obtains,

$$\sigma_s \text{ step} = 28.8 \text{ ns/km} \quad \text{and} \quad \sigma_s \text{ graded} = 0.057 \text{ ns/km}$$

Because of its substantially improved performance, graded index multimode fiber is the clear choice when one wants to exploit the advantages of the multimode fiber with low intermodal dispersion.

### To summarise, dispersion can be reduced in the following ways:

1. Single mode fibers eliminate modal dispersion.
2. Operation at  $\lambda_0$  (zero dispersion wavelength) eliminates material dispersion at the single  $\lambda_0$  but not over the complete spectrum.
3. For  $\lambda > \lambda_0$ , the zero dispersion  $\lambda$  can be shifted to longer wavelength by matching  $-D_w$  by  $+D_m$  at that  $\lambda$ .
4. By using a complex refractive index profile, a low total dispersion over a wide range of wavelength is possible.

### To analyse beam propagation in graded index fiber:

Some assumptions are required to be considered:

1. The refractive index profile is circularly symmetric.
2. The fiber is a multimode fiber with a large core diameter such that  $a > 50 \mu\text{m}$ .
3. The total index change within guiding core region is small ( $\Delta \ll 1$ ) so that the modes can be considered transverse electromagnetic.
4. Index variations are very small over distances of a wavelength so that the conditions of geometric optics apply.

With the help of these assumptions, we solve,

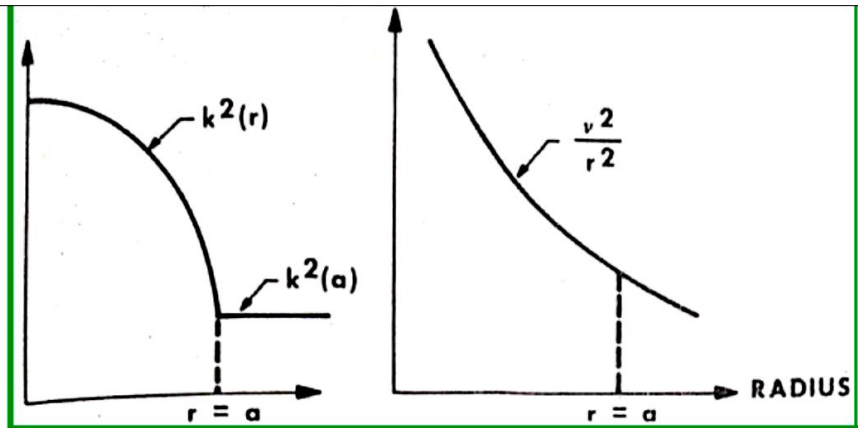
$$\frac{\partial^2 E_z}{\partial r^2} + \frac{1}{r} \frac{\partial E_z}{\partial r} + \frac{1}{r^2} \frac{\partial^2 E_z}{\partial \phi^2} + \xi^2 E_z = 0$$

It can be shown that for a propagating mode to exist in a graded index fiber,

$$\xi^2 - \frac{v^2}{r^2} > 0 \quad \text{and} \quad k^2(r) - \beta^2 - \frac{v^2}{r^2} > 0 \quad (8)$$

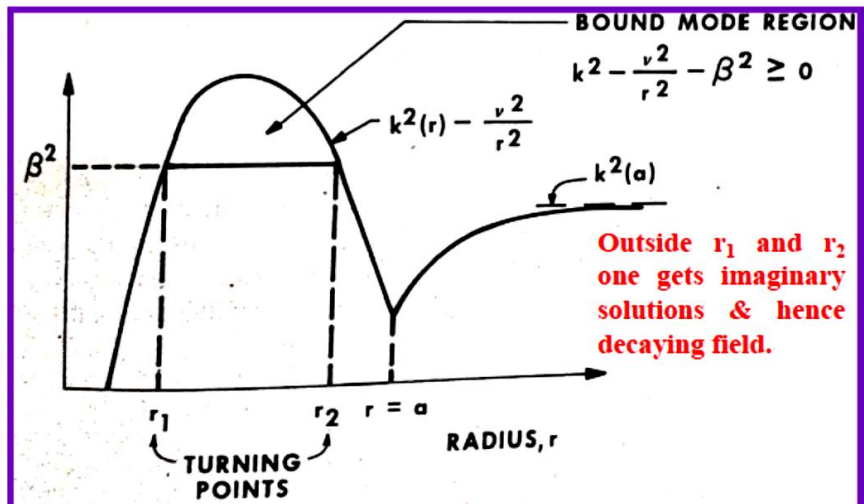
Here propagation constant  $k$  has now become a function of  $r$  as we are considering graded index fiber.

Since at  $r = a$ ,  $n(r) = n_2$  and so also for  $r > a$ , i.e. a constant value, hence  $k^2(a)$  is constant. The beam is now in the cladding.

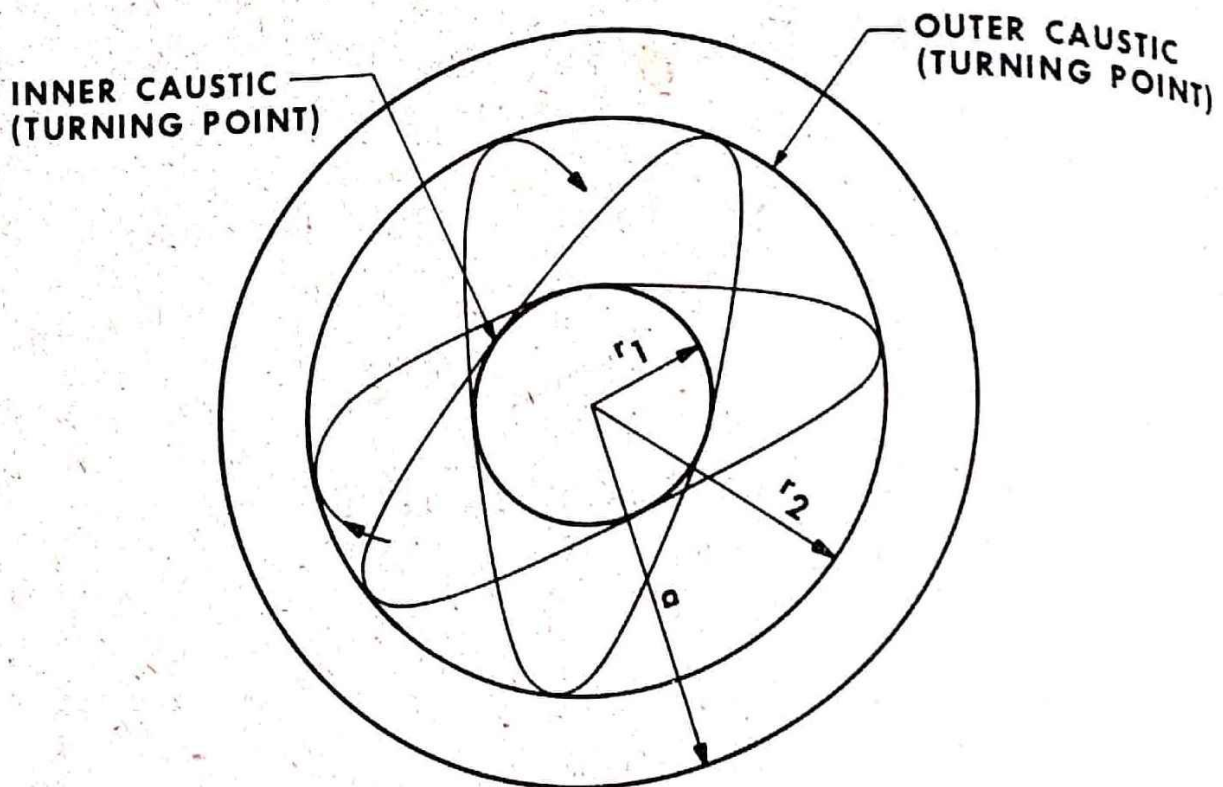


For a given  $\beta$ , at two values of  $r$  ( $r_1$  and  $r_2$ ),  $k^2(r) - \beta^2 - \frac{v^2}{r^2} = 0$

Since at  $r = 0$ , both  $k^2(r)$  and  $v^2/r^2$  are high, hence their difference is  $\sim 0$  in the initial stage.



For  $\beta$  value fixed and  $v$  increases, the region between the two CAUSTICS becomes narrower. As  $v$  is increased further, a point will be reached where the CAUSTICS merge. Beyond this point the wave is no longer bound. Thus propagation conditions of a wave depend on the values of both  $\beta$  and  $v$ . And what we get are hybrid modes as shown:



## Source coupling into an optical fiber:

If  $P_F \Rightarrow$  Power injected into the fiber

$P_S \Rightarrow$  Output power of the source

$\eta_C \Rightarrow$  Coupling efficiency of a source into an optical fiber

$$= \frac{P_F}{P_S}$$

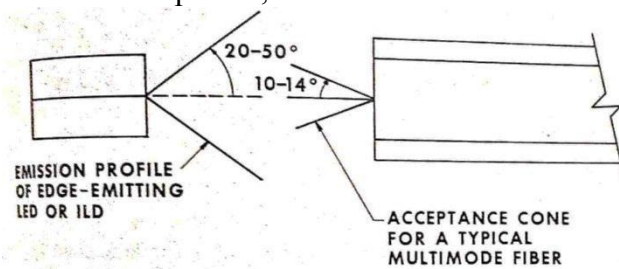
$\eta_C$  depends on:

(i) **Unintercepted illumination loss**

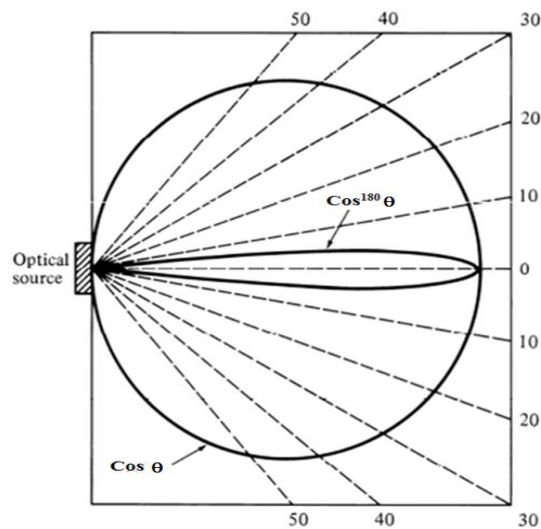
- Area mismatch between source spot size & fiber core area
- Misalignment of source and fiber axes

(ii) **Numerical aperture loss**

Caused by that part of the source emission profile, that radiates outside of the fiber's acceptance angle.

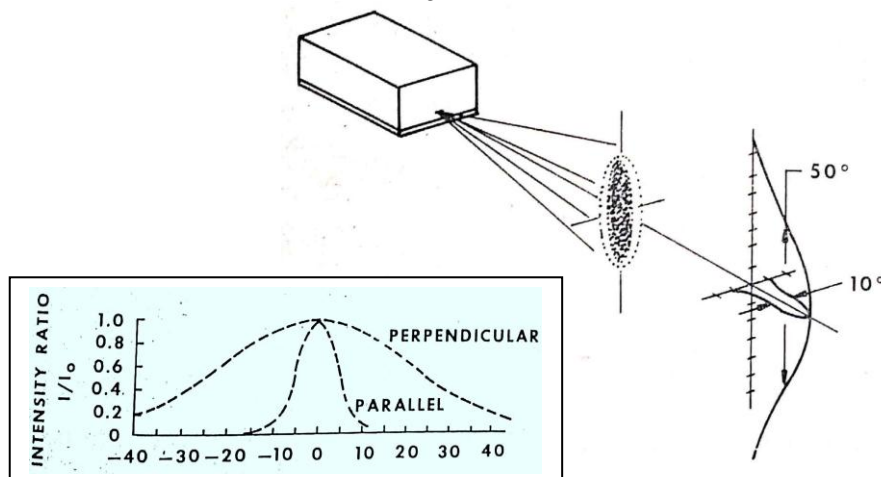


**NUMERICAL APERTURE MISMATCH OF SOURCE AND MULTIMODE FIBER**



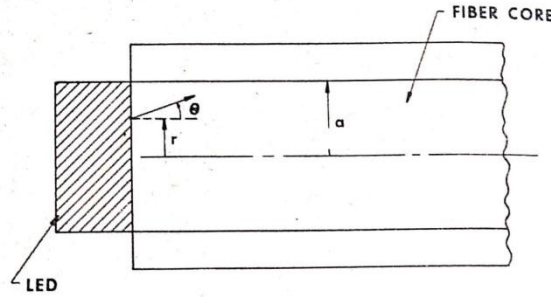
**Surface emitting LEDs have a Lambertian output pattern**

**Far field radiation pattern of Injection Laser Diode (ILD)**



**We consider:**

1. Multimode graded index fiber.
2. The source (LED) has Lambertian profile.
3. The source is in direct contact with the fiber core covering the latter's entire cross-section.



Each element  $dA$  radiates amount of power  $\Delta P$  in the  $\theta$  direction as,

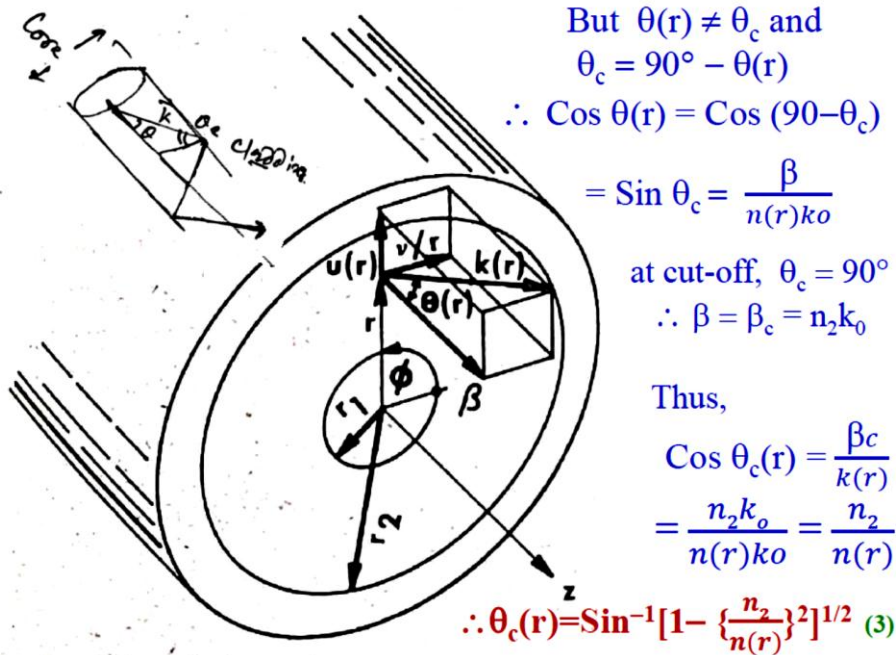
$$\Delta P = B \cos\theta \, dA \, d\Omega \quad (1)$$

$B \cos\theta \Rightarrow$  the brightness of the Lambertian radiation

$d\Omega \Rightarrow$  element of solid angle =  $\sin\theta \, d\theta \, d\phi$

$dA \Rightarrow$  element of surface area =  $r \, dr \, d\theta$

Due to numerical aperture mismatch, not all the radiation will enter inside the fiber. The source angles that are too steep to be trapped inside will go to cladding. The trapping angle of the energy from the source into the fiber at each position  $r$  in the fiber core is obtained if we consider the ray angle (i.e. energy propagation direction) associated with a given mode at cut-off.



Hence, the total power the LED injects:

$$\begin{aligned}
 P_f &= \int_{A_f} [ \int_{\Omega_f} B \cos\theta \, d\Omega_s ] \, dA_s \\
 &= B \int_0^a r \, dr \int_0^{2\pi} d\phi \int_0^{2\pi} d\theta' \int_0^{\theta_c(r)} \sin\theta \cos\theta \, d\theta \\
 &= 2\pi B \int_0^a r \, dr \int_0^{2\pi} \frac{1}{2} \sin^2\theta_c(r) \, d\theta' \\
 &= \pi B \int_0^a r \, dr \int_0^{2\pi} (NA)^2 \, d\theta' \\
 &= \pi^2 a^2 B (NA)^2
 \end{aligned}$$

$$P_f |_{\text{step}} \approx 2\pi^2 a^2 B n_1^2 \Delta \quad (4)$$

For graded index fiber one uses usual power profile description of  $n(r)$

$$n(r) = \begin{cases} n_1(1 - 2\Delta(r/a)^\alpha)^{1/2} & r < a \text{ core} \\ n_1(1 - 2\Delta)^{1/2} = n_2 & r \geq a \text{ cladding} \end{cases}$$

And use it in eq.(3) which will then yield,

$$P_f|_{\text{multi}} \approx 2\pi^2 a^2 B \Delta \frac{\alpha}{\alpha+2} \quad (5)$$

Total optical power from source,

$$P_s = A_s B \int_0^{2\pi} d\phi \int_0^{\pi/2} \sin\theta \cos\theta d\theta$$

$$= \pi a^2 2\pi B (1/2)$$

$$P_s = \pi^2 a^2 B \quad (6)$$

$$\therefore \eta_c = \frac{P_f}{P_s} = \frac{2\alpha\Delta}{\alpha+2}$$

For a parabolic index profile,  $\alpha = 2$  and hence,

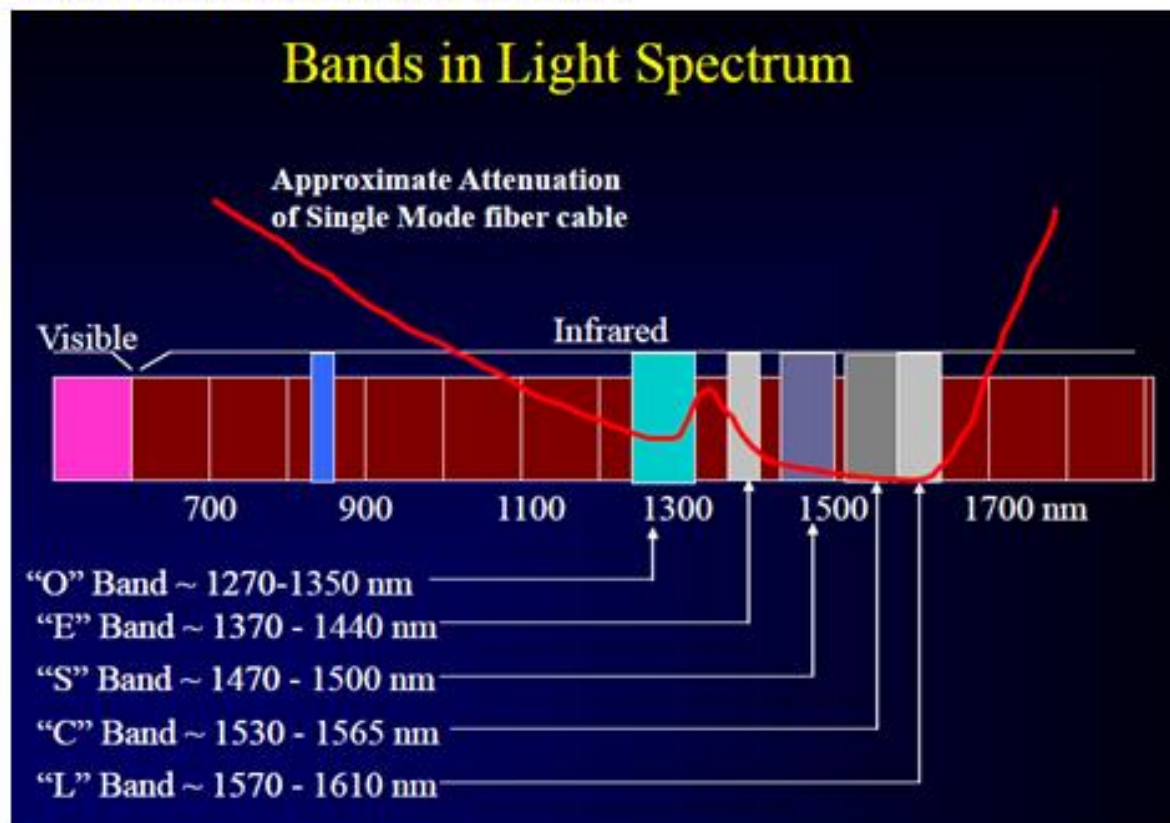
$$\eta_c|_{\text{parabolic}} = \Delta$$

For a step index profile,  $\alpha = \infty$  and hence,

$$\eta_c|_{\text{parabolic}} = 2\Delta$$

Hence, the coupling efficiency of a step index fiber is twice that of a parabolic index fiber.

## TRANSMISSION WINDOWS





## Fiber Optic Loss Calculations:

$$\text{Loss} = \frac{P_{out}}{P_{in}} = \frac{\text{Input power to the fiber}}{\text{power available at the output of the fiber}} \quad (8.1)$$

Fiber optic loss is typically expressed in terms of decibels (dB)

$$\text{Loss}_{dB} = 10 \log \frac{P_{out}}{P_{in}} \quad (8.2a)$$

The loss is also expressed in terms of dB/km.

A communication system uses 10 km of fiber that has a 2.5-dB/km loss characteristic. Find the output power if the input power is 400 mW.

One knows that if  $x = \log y$ , then  $y = 10^x$ . Using this relation in eq.(8.2a),

$$\text{Loss}_{dB} = 10 \log \left( \frac{P_{out}}{P_{in}} \right)$$

$$\frac{\text{Loss}_{dB}}{10} = \log \left( \frac{P_{out}}{P_{in}} \right)$$

which becomes, then,

$$10^{\frac{\text{Loss}_{dB}}{10}} = \left( \frac{P_{out}}{P_{in}} \right).$$

So, finally, we have

$$P_{out} = P_{in} \times 10^{\frac{\text{Loss}_{dB}}{10}} \quad (8-2b)$$

For 10 km of fiber with 2.5-dB/km loss characteristic, the loss<sub>dB</sub> becomes

$$\text{Loss}_{dB} = 10 \text{ km} \times (-2.5 \text{ dB/km}) = -25 \text{ dB}$$

Plugging this back into Equation 8-2b,

$$P_{out} = (400 \text{ mW}) \times 10^{\frac{-25}{10}} = 1.265 \text{ mW}$$

The performance of a digital lightwave system is characterized through the **biterror rate** (BER). It is customary to define the BER as *the average probability of incorrect bit identification*. Therefore,  $\text{BER} \sim 10^{-6} \Rightarrow$  on average 1 error per million bits. Most lightwave systems specify a  $\text{BER} \sim 10^{-9}$  as the operating requirement; some even need a  $\text{BER} \sim 10^{-14}$ . The error-correction codes are sometimes used to improve the raw BER of a lightwave system. An important parameter for any receiver is the **receiver sensitivity**. It is usually defined as *the minimum average optical power required to realize a BER of  $10^{-9}$* . Receiver sensitivity depends on the signal to noise ratio (SNR), which in turn depends on various noise sources that corrupt the signal received. Even for a perfect receiver, some noise is introduced by the process of photo-detection itself which is the *quantum noise* or the *shot noise*, as it has its **origin in the particle nature of electrons**.

The decision circuit compares the sampled value with a threshold value  $I_D$  and calls it bit 1 if  $I > I_D$  or bit 0 if  $I < I_D$ . An error occurs if  $I < I_D$  for bit 1 because of receiver noise. An error also occurs if  $I > I_D$  for bit 0. Both sources of errors can be included by defining the *error probability* as

$$\text{BER} = p(1)P(0/1) + p(0)P(1/0)$$

where  $p(1)$  &  $p(0)$  are the probabilities of receiving bits 1 and 0, respectively,  $P(0/1)$  is the probability of deciding 0 when 1 is received, and  $P(1/0)$  is the probability of deciding 1 when 0 is received. Since 1 and 0 bits are equally likely to occur,  $p(1)=p(0)=1/2$  and the BER becomes

$$\text{BER} = \frac{1}{2}[P(0/1) + P(1/0)]$$

Fig 1(b) below shows how  $P(0/1)$  &  $P(1/0)$  depend on the probability density function  $p(I)$  of the sampled value  $I$ . The functional form of  $p(I)$  depends on the statistics of noise sources responsible for current fluctuations.

The receiver sensitivity is then defined as the minimum average received power  $P_{rec}$  required by the receiver to operate at a BER of  $10^{-9}$ .

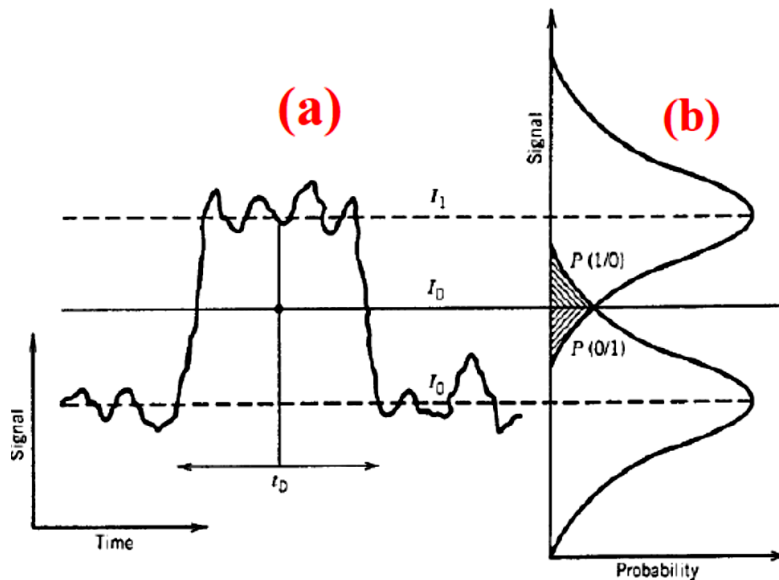
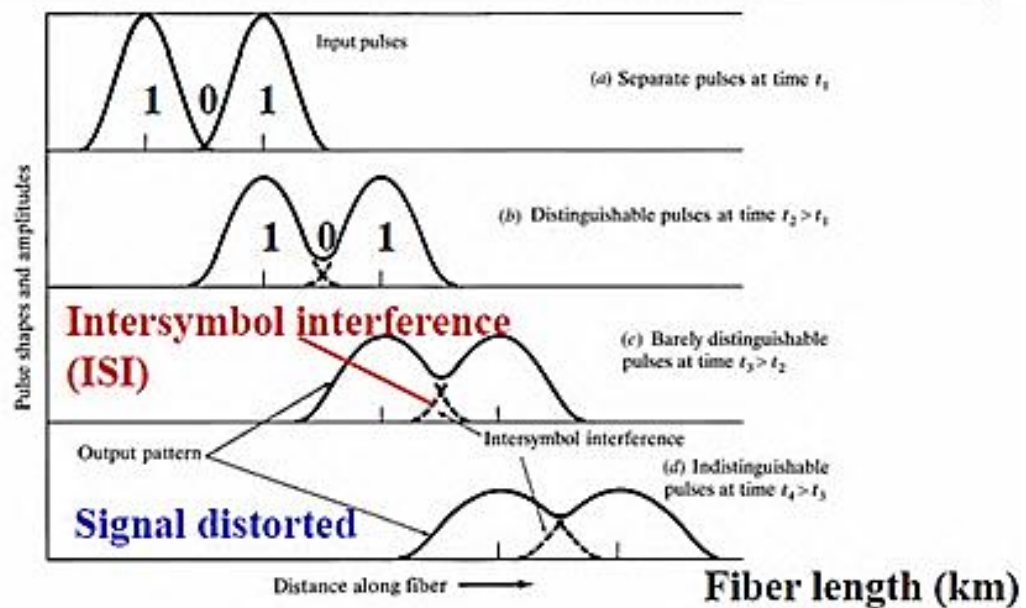


**Figure 1:**

(a) Fluctuating signal generated at the receiver and received by the decision circuit, which samples it at the decision instant  $t_D$  determined through clock recovery. The sampled value  $I$  fluctuates from bit to bit around an average value  $I_1$  or  $I_0$ , depending on whether the bit corresponds to 1 or 0 in the bit stream.

(b) Gaussian probability densities of 1 & 0 bits. The dashed region shows the probability of incorrect identification.

## Pulse broadening limits fiber bandwidth (data rate)



- An *increasing number of errors* may be encountered on the digital optical channel as the ISI becomes more pronounced.

## How does modal dispersion restricts fiber bit rate?

e.g. How much will a light pulse spread after traveling along 1 km of a step-index fiber whose NA = 0.275 and  $n_{\text{core}} = 1.487$ ?

Suppose we transmit at a low bit rate of 10 Mb/s

=> Pulse duration =  $1 / 10^7 \text{ s} = 100 \text{ ns}$

Using the above e.g., each pulse will spread up to  $\approx 100 \text{ ns}$  (i.e.  $\approx$  pulse duration !) every km

=>The broadened pulses overlap! (**Intersymbol interference (ISI)**)

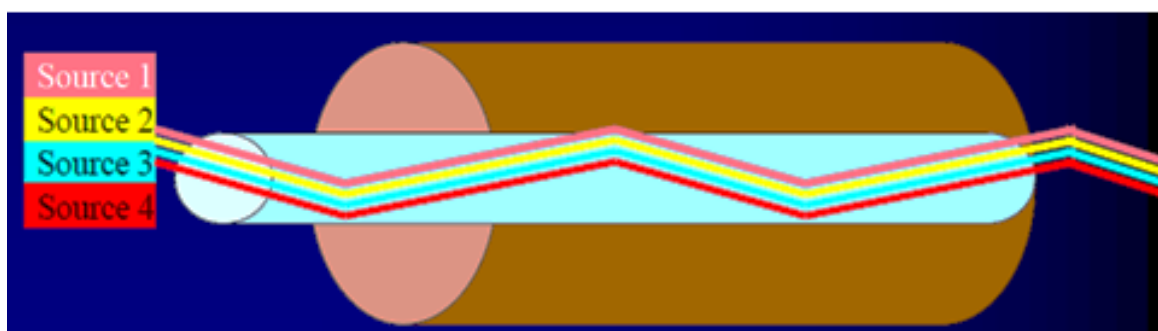
\*Modal dispersion limits the bit rate of a km-length fiber-optic link to  $\sim 10 \text{ Mb/s}$ . (a coaxial cable supports this bit rate easily!)

### Multiplexing:

*Whenever the bandwidth of a medium linking two devices is greater than the bandwidth needs of the devices, the link can be shared. Multiplexing is the set of techniques that allows the simultaneous transmission of multiple signals across a single data link. As data and telecommunications use increases, so does traffic.*

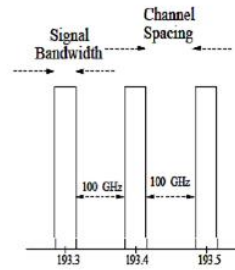
#### Wavelength Division Multiplexing

- The technology of using multiple optical signals on the same fiber is called *wavelength division multiplexing (WDM)*.
- WDM Optical Network
  - Divide the vast transmission bandwidth available on a fiber into several different smaller capacity “channels” – non-overlapping bandwidths,
  - Each of these channels can be operated at a moderate bit rate (2.5-40 Gb/s) that electronic circuits can handle,
  - Each of these channels corresponds to a different carrier wavelength.



## Channel spacing or guard band in WDM

- In WDM networks, each signal on a fiber is given a fixed bandwidth.
- In order to avoid interference between signals, a fixed spacing is maintained between signals using adjacent bandwidths, called as “guard band”.
- Signal Bandwidth = 10 GHz
- Channel Spacing = 100 GHz

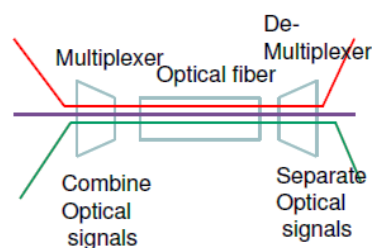


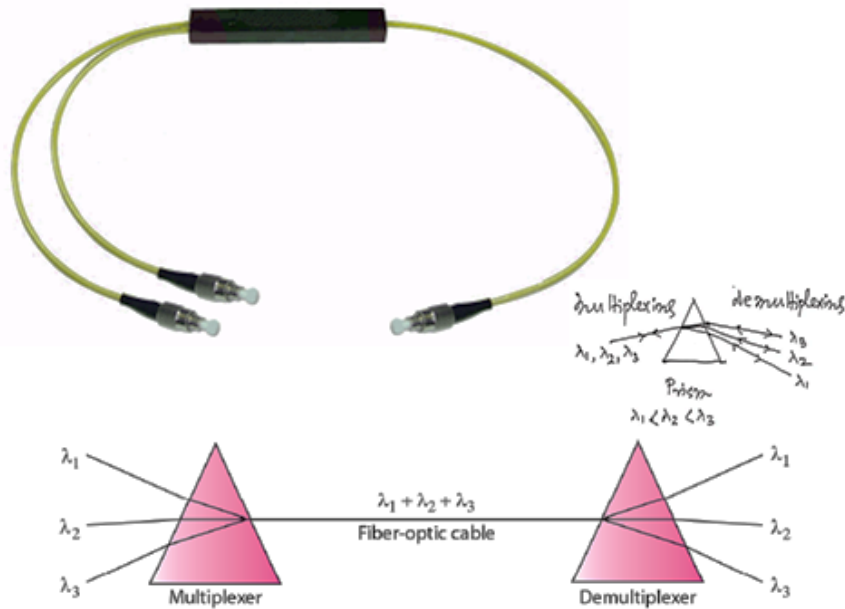
## Data Transmission in WDM networks

- Carrier Frequency:
- Digital Data:
- Modulated signal:

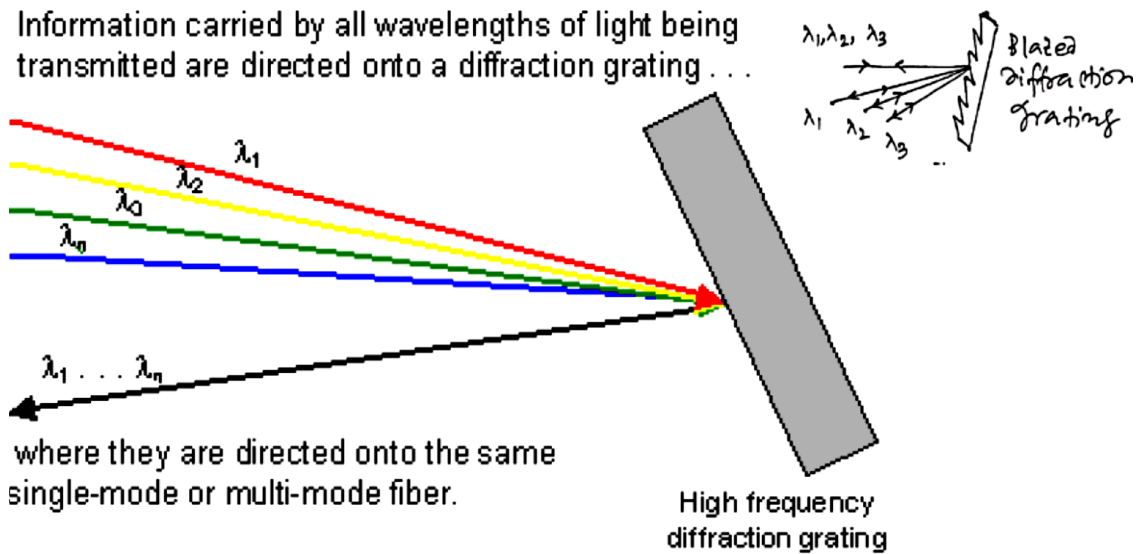
## What do we need to achieve WDM Communication

- Transmitter – convert data to a modulated optical signal
- Receiver – Convert a modulated optical signal to data
- Multiplexer – to combine multiple optical signals
- Demultiplexer – to separate signals having different carrier wavelengths
- Routers – to direct the signals from the source to the destination
- Add- drop multiplexers – to add new signals to a fiber and extract some signals



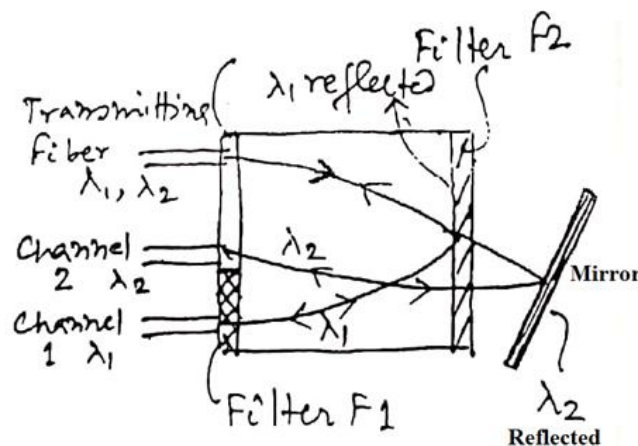


Information carried by all wavelengths of light being transmitted are directed onto a diffraction grating . . .

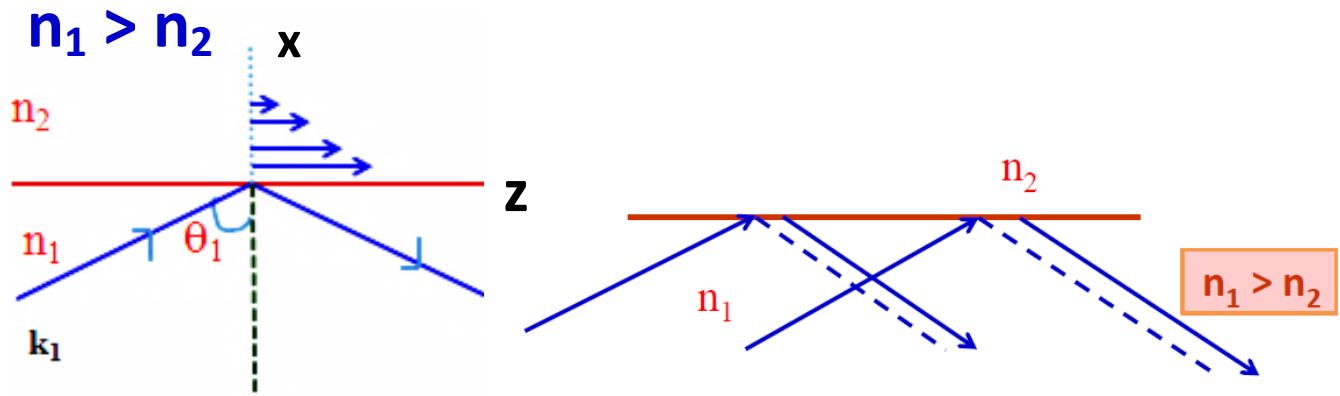


where they are directed onto the same single-mode or multi-mode fiber.

Reflection gratings can also be used to separate wavelengths. By choosing a suitable periodic structure for the grating, it is possible to coincide the directions of constructive interference and specular reflection from the grating for a given order and wavelength. The technique is known as **blazing**.

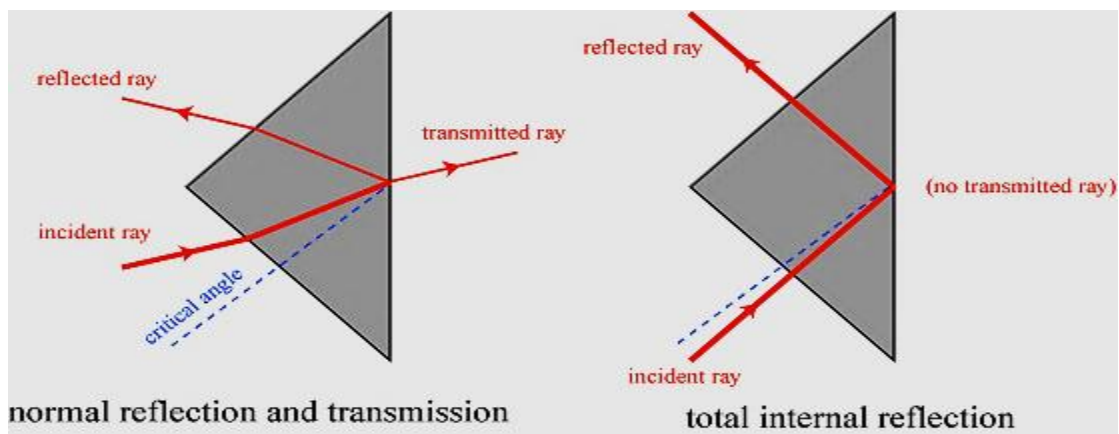


**EVANESCENT WAVE (The concept is required for Directional Couplers):**

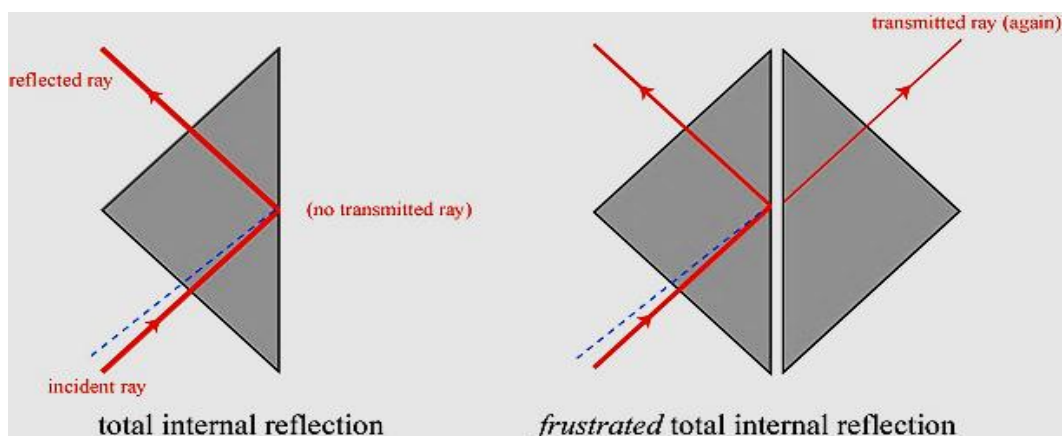


Although due to total internal reflection, the entire energy is reflected back, there is power flowing in the second medium (with r.i.  $n_2$ ). Physically we can understand this by considering the incidence of a spatially bound beam at the interface (fig next). As shown, the beam undergoes a lateral shift. This can be interpreted as the beam entering the rarer medium and reemerging from the rarer medium after reflection. **This shift is known as the Goos-Hanchen shift.** It is now physically obvious that if, instead of a spatially bounded beam, we have an infinitely extended plane wave incident on the interface then although the reflection is complete, energy will flow along the  $z$ -axis in the rarer medium, the magnitude of this energy decays along  $x$ -axis.

It was first studied in detail by none other than the great [Sir Isaac Newton](#), who used a prism to study the effect. An illustration of how this might have worked is shown below.

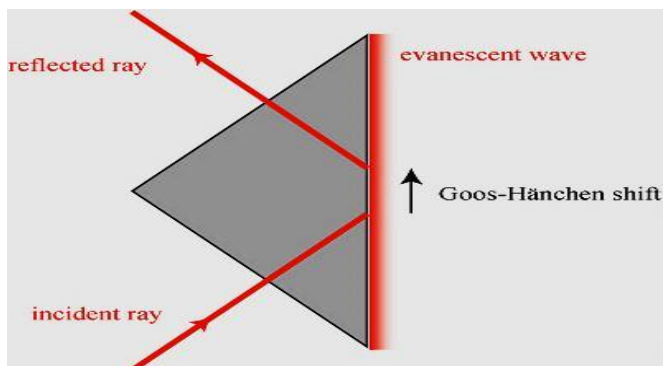


The thickness of the rays is supposed to indicate their brightness. In the normal reflection case, part of the light gets reflected, part gets transmitted. In the total internal reflection case, all gets reflected. But Newton noticed something else — when a second prism is brought really close and parallel to the first one, light starts to get transmitted again!

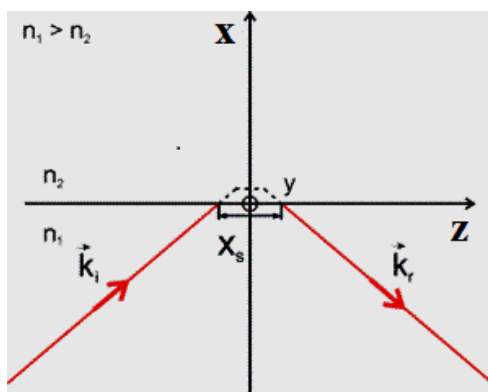


This process, known as **frustrated total internal reflection (FTIR)**, only occurs when the second prism is brought **within a distance comparable to the wavelength of the light being used**. In the case of visible light, this wavelength is about 0.0005 mm or 500 nm, a very small number!

If one looks at the images that have been drawn of total internal reflection above, it have been shown the reflected ray bouncing off of the glass **at the same point** where the incident ray hits. However, when one does a rigorous theoretical analysis of the reflection, one finds that the picture should really look as follows.



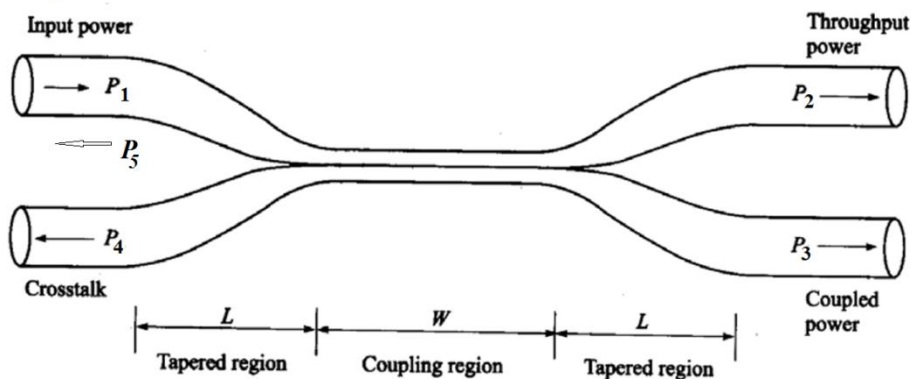
A beam of light, reflected off of a surface in total internal reflection, ends up being reflected from a point further along than where the incident field hits! This is the Goos-Hänchen shift. F. Goos and H. Hänchen reported the definitive experimental observation of this effect in their 1947 paper, “Ein neuer und fundamentaler Versuch zur Totalreflexion,” or “A new and fundamental test for total reflection.”



Dashed line in the figure shows in a very symbolic way the direction of propagation of the evanescent wave.

The hypothesis is that the light, instead of immediately reflecting at the surface of the glass, instead converts to an evanescent wave and “creeps” along the outer surface before becoming a reflected wave. Because evanescent waves only exist in the case of total internal reflection, this seemed like a plausible explanation.

## 2x2 or Four Port Directional Coupler:



$P_1$  is the input power,  $P_2$  is the throughput power, and  $P_3$  is the power coupled into the second fibre. The parameters  $P_4$  and  $P_5$  are extremely low signal levels resulting from backward reflections and scattering.

As the input light  $P_1$  propagates along the taper in fibre 1 and into the coupling region  $W$ , there is a significant decrease in the  $V$  number owing to the reduction in the ratio  $r/\lambda$ , where  $r$  is the reduced fibre radius.

As the signal enters the coupling region, an increasingly larger portion of the input field now propagates outside the core of the fibre. Depending on the dimensioning of the coupling region, any desired fraction of this decoupled field can be recoupled into the other fibre. These devices are also known as *directional couplers*.

2. Throughput loss:  $L_{THP} = -10 \log \frac{P_2}{P_1}$   
 Specifies amount of transmission loss between the input port and the favoured port (2).

2. Tap loss:  $L_{TAP} = -10 \log \frac{P_3}{P_1}$  Tap port  
Input port

3. Directionality:  $L_D = -10 \log \frac{P_4}{P_2}$   
 Specifies the loss between the input port and the port we wish to isolate (4).

4. Excess loss:  $L_E = -10 \log \frac{P_2 + P_3}{P_1}$   
 Specifies the power lost within the coupler. It includes radiation, scattering, absorption and coupling to the isolated port.

In an ideal coupler (i)  $P_4 = 0$ .  $\therefore L_D \rightarrow \infty$  as  $\log 0 = -\infty$

(ii) no power is lost  $\therefore P_3 + P_2 = P_1$

i.e.  $L_E = 0$

Good DC's have  $L_E < 1$  dB and  $L_D > 40$  dB. (i.e.  $P_4/P_2 = 0.0001$ )

$P_2/P_3$  is the splitting ratio, couplers are often described by their tap loss. A 10 dB coupler is one

that has a 10 dB tap loss.

Coupler description	$L_{TAP}$ (dB)	$L_{THP}$ (dB)	Splitting ratio ( $P_2/P_3$ )
3 dB	3	3	1:1
6 dB	6	1.25	3:1
10 dB	10	0.46 <sup>+</sup>	9:1 <sup>++</sup>
12 dB	12	0.28	15:1



For lossless couplers,

$$P_2 = P_1 - P_3$$

Hence  $L_{THP}$  can be expressed as,

$$L_{THP} = -10 \log (1 - 10^{-L_{TAP}/10})$$

\* A coupler has  $L_E = 1$  dB and a splitting ratio 1:1. How much of the input power reaches the two output terminals?

Since splitting ratio is 1:1  $\therefore P_2 = P_3$ .

$$L_E = -10 \log \frac{P_2 + P_3}{P_1} = -10 \log \frac{2P_2}{P_1} = 1 \text{ dB.}$$

$$\therefore P_2/P_1 = P_3/P_1 = 0.397. \quad \therefore 2P_2/P_1 = 10^{-1/10} = 0.794$$

$$\therefore L_{THP} = -10 \log P_2/P_1 = -10 \log 0.397 = 4 \text{ dB.}$$

$$L_{TAP} = -10 \log P_3/P_1 = -10 \log 0.397 = 4 \text{ dB}$$

[It is seen that the losses exceeds the losses of an ideal coupler having the same splitting ratio (3dB), by 1dB, the excess loss itself.]

The coupler is bidirectional. Any of the four ports can serve as the input. Possible couplings are:

$$1 \rightarrow 2, 3$$

$$2 \rightarrow 1, 4$$

$$3 \rightarrow 4, 1$$

$$4 \rightarrow 3, 2$$

Directional couplers are normally constructed symmetrically, so the characteristic losses have the same values regardless of which port is chosen as the input.

\* Also,  $P_3 = P_1 10^{-L_{TAP}/10}$  from tap loss definition

if  $L_{TAP} = 10$  dB then,

$$P_3 = P_1/10 = 0.1 P_1$$

$$\therefore P_2 = P_1 - P_3 = 0.9 P_1$$

$$\therefore P_2/P_3 = 9:1$$

[for 10dB coupler  $\rightarrow -10 \log (1 - 10^{-10/10}) = -10 \log (1 - 1/10) = -10 \log 0.9$

$= (-10) \cdot (-0.046) = +0.46$

## WHAT IS AN OTDR?

A measurement technique which provides the loss characteristics of an optical link down its entire length giving information on the length dependence loss.

- Also allows splice and connector losses to be evaluated as well as location of any faults on the link.
- Also called **backscatter measurement method**.
- It relies upon the measurement & analysis of the fraction of light which is reflected back within the fiber's numerical aperture due to *Rayleigh scattering within the fiber*.
- A small proportion of the scattered power is collected by the fiber in backward direction and returns to the transmitter, where it is measured by a photodiode.

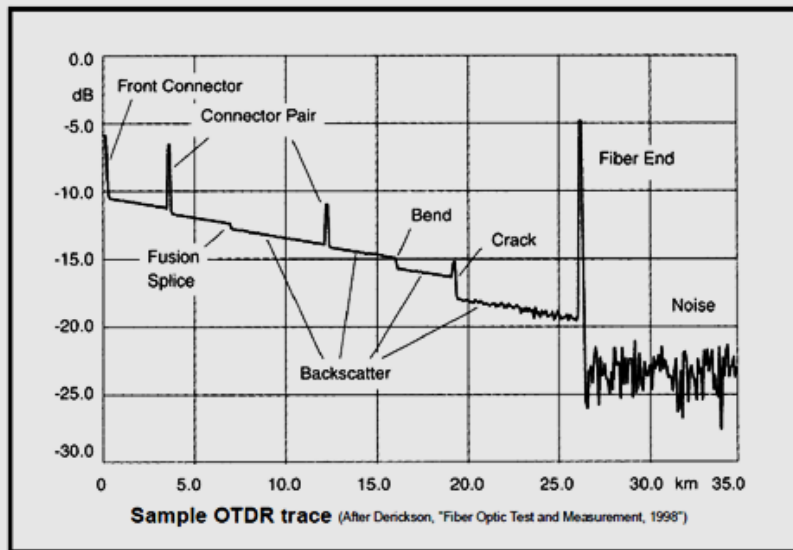
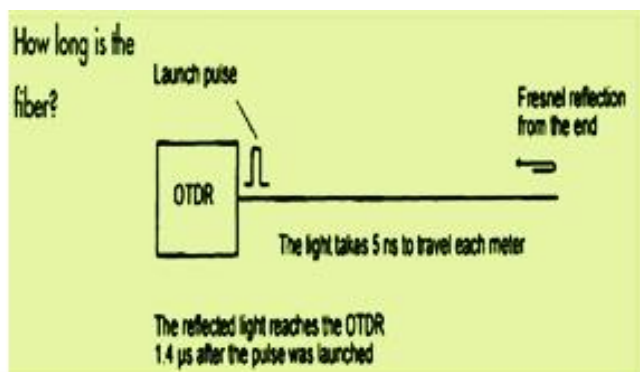


Figure 2



- Consider the Refractive index of the core  $n_1=1.5$
- Then the speed of light in the core  $=V=c/n_1=2 \times 10^8$  m/s
- If the Reflected Light reaches the OTDR 1.4 μs later
- Since the Light has travelled back and forth along the length of the fiber(L)
- $2L=V \times \text{delay time}$
- $2L=2 \times 10^8 \times 1.4 \mu\text{s}=280\text{m}$
- Hence  $L=140\text{m}$
- Hence the OTDR uses the principle of RADAR .It sends a optical pulse and then listens to the ECHO

## Evolution of fiber Optic system

### First generation

- The first generation of light wave systems uses GaAs semiconductor laser and operating region was near  $0.8\ \mu\text{m}$ . Other specifications of this generation are as under:
- i) Bit rate : 45 Mb/s
- ii) Repeater spacing : 10 km

### Second generation

- i) Bit rate: 100 Mb/s to 1.7 Gb/s ii) Repeater spacing: 50 km
- iii) Operation wavelength:  $1.3\ \mu\text{m}$  iv) Semiconductor: In GaAsP

### Third generation

- i) Bit rate : 10 Gb/s
- ii) Repeater spacing: 100 km
- iii) Operating wavelength:  $1.55\ \mu\text{m}$

### Fourth generation

- Fourth generation uses WDM technique. i) Bit rate: 10 Tb/s
- ii) Repeater spacing:  $> 10,000\ \text{km}$
- Iii) Operating wavelength:  $1.45$  to  $1.62\ \mu\text{m}$

### Fifth generation

- Fifth generation uses Raman amplification technique and optical solitons. i) Bit rate: 40 - 160 Gb/s
- ii) Repeater spacing: 24000 km - 35000 km iii) Operating wavelength:  $1.53$  to  $1.57\ \mu\text{m}$

### *Some Reference Books:*

1. *An introduction to Optical Fibers, Allen H Cherin, McGraw-Hill College.*
2. *Introduction to Fiber Optics, A Ghatak and K Thyagarajan, Cambridge University Press.*
3. *Optical Electronics, A K Ghatak and K Thyagarajan, Cambridge University Press.*
4. *Optical Fibers, Cables and Systems, ITU-T Manual (2010), International Telecommunication Union.*

# Nonlinear Optics:

(Discussion will be limited to effects due to  $\chi^{(2)}$  only)

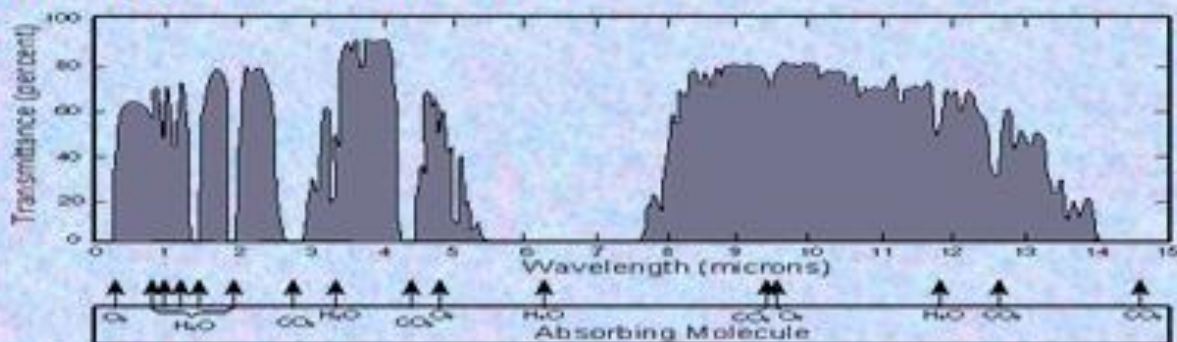
The impact of NLO on science:

- Optical nonlinearities: Crystals, amorphous materials, polymers, liquid crystals, semiconductors, organics, liquids, gases and plasmas.
- OPO: Extends tunability to a large extent.
- THz Generation.
- SRS can turn silicon into an emitter, when pumped external to the silicon chip. Japanese researchers have recently reported  $\mu\text{W}$ -threshold Raman lasers in silicon with  $\mu\text{m}$ -scale geometry.
- Ultra short pulse generation & Solitons.
- Recently, ps and fs pulses have been used for laser machining since the ablation and hole-digging process can be very clean owing to elimination of thermal effects that cause microcracks and molten debris.

Apart from different spectroscopic applications widely tunable coherent radiation have many other uses. For example, drinking water can be disinfected from bacteria and protozoan by causing permanent damage to their DNA through irradiation of ultraviolet (UV) radiation. Furthermore, dose of UV intensity as high as  $16000 \mu\text{W}\cdot\text{s}/\text{cm}^2$  may be needed for total destruction of some protozoan cysts like giardia. Except excimer lasers, there is no such high power UV lasers. However, excimer lasers have limited life and they are also quite hard to operate.

Again most of the trace atmospheric constituents of environmental interest have their fingerprints in the infrared (IR) region. And coherent radiation at both the atmospheric window regions, namely  $3\text{--}5 \mu\text{m}$  and  $8\text{--}12 \mu\text{m}$ , are widely used for spectroscopic analysis of such trace gases.

## Atmospheric Windows



**3-5  $\mu\text{m}$ :** Trace Gas Analysis as it is the Fingerprint region of trace gases.

**& 8-12  $\mu\text{m}$ :** Infrared Detectors on satellites measure the relative amount of infrared radiation from the ground in this wavelength band in order to provide an indication of the ground temperature.

## 16 $\mu\text{m}$ radiation

Laser isotope separation — particularly isotopes of uranium. Spectral coincidence of the laser emission with an absorption line of a single isotope. A strong absorption band of uranium hexafluoride ( $\text{UF}_6$ ) is centered at a wavelength of approximately  $16 \mu\text{m}$ .

# First Demonstration of Optical Harmonic Generation

VOLUME 7, NUMBER 4

PHYSICAL REVIEW LETTERS

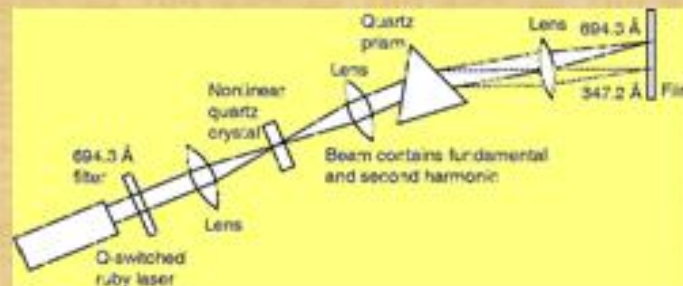
AUGUST 15, 1961

## GENERATION OF OPTICAL HARMONICS\*

P. A. Franken, A. E. Hill, C. W. Peters, and G. Weinreich

The Harrison M. Randall Laboratory of Physics, The University of Michigan, Ann Arbor, Michigan  
(Received July 21, 1961)

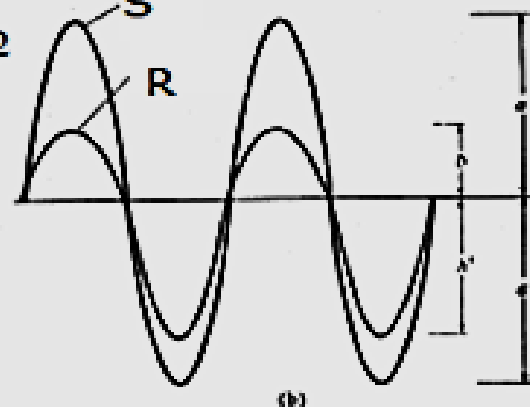
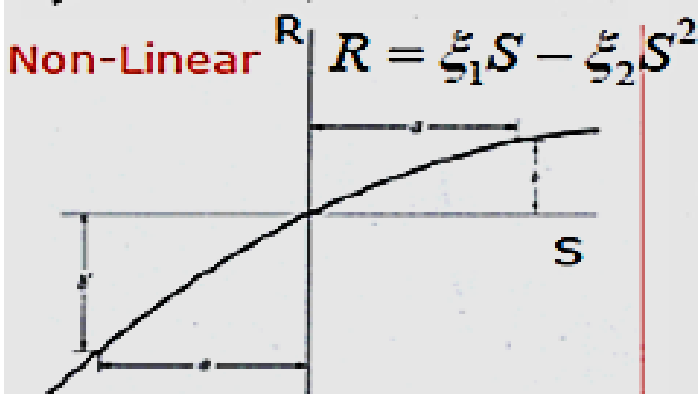
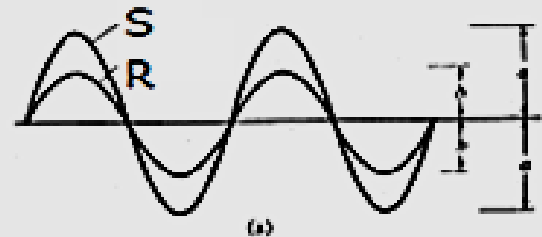
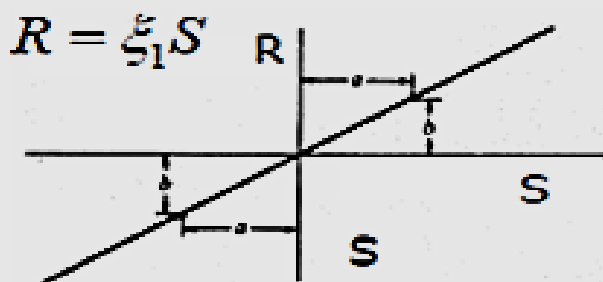
- Ruby Laser:  $\lambda = 694.3 \text{ nm}$ ;  $P = 3 \text{ J}$ ;  $\tau = 1 \text{ ms} \Rightarrow E \sim 10^5 \text{ V/cm}$
- Quartz Sample: no phase matching
- Output analyzed with prism spectrometer/photographic plate



One of the very important gifts of Nonlinear Optics is the Frequency Conversion Technique to expand the usefulness of the existing lasers by covering the gaps within the offered tunability.

## Representation of Nonlinearity

### Linear





*Calculated  $\chi^{(1)}$  with the electron modeled as a harmonic oscillator.*

*Hendrik Antoon Lorentz (1853-1928)*

*“Lorentz lacked the stimulation from stimulated emission of radiation.”*

*—Nobel Lecture (1981)*

*Nicolaas Bloembergen (1920-2017)*



## Introduction:

Nonlinear optical devices are based on the nonlinear response of the dielectric material polarization to an applied strong electro-magnetic field. The dielectric material polarization  $\mathbf{P}$  is defined as the induced dipole moment per unit volume. According to the classical model of Lorentz, due to an applied electro-magnetic (EM) field  $\mathbf{E}$  in a material,  $\mathbf{P}$  will be given by,

$$\mathbf{P} = \epsilon_0 \chi^{(1)} \mathbf{E} \quad (1)$$

with the linear susceptibility  $\chi^{(1)}$ . When the applied field is so intense that it is of the same order of magnitude as the interatomic fields, the electrons start anharmonic oscillations and the anharmonic terms will appear in the induced polarization of the material as.

$$\mathbf{P}_{\text{total}} = \epsilon_0 (\chi^{(1)} \mathbf{E} + \chi^{(2)} \mathbf{E}^2 + \chi^{(3)} \mathbf{E}^3 + \chi^{(4)} \mathbf{E}^4 + \dots) \quad (2)$$

where  $\chi^{(1)} \mathbf{E} \gg \chi^{(2)} \mathbf{E}^2 \gg \chi^{(3)} \mathbf{E}^3$  and so on. In this article, we will consider the effects of the first nonlinear component of the polarization only which is,

$$\mathbf{P}_{\text{NL}}^{(2)} = \epsilon_0 \chi^{(2)} \mathbf{E}^2 = 2d \epsilon_0 \mathbf{E}^2 \quad (3)$$

Consider e.g., two traveling waves  $\mathbf{E}_1$  and  $\mathbf{E}_2$ : given as,

$$\mathbf{E}_1(z,t) = \mathbf{E}_1 \cos(\omega_1 t + k_1 z) \quad (4)$$

$$\mathbf{E}_2(z,t) = \mathbf{E}_2 \cos(\omega_2 t + k_2 z) \quad (5)$$

When substituted in eq. 3, their interaction will result in the following nonlinear polarization:

$$\begin{aligned} \mathbf{P}_{\text{NL}}^{(2)} = 2d \epsilon_0 [ & \mathbf{E}_1^2 \cos(\omega_1 t + k_1 z) + \mathbf{E}_2^2 \cos(\omega_2 t + k_2 z) \\ & + 2 \mathbf{E}_1 \mathbf{E}_2 \cos(\omega_1 t + k_1 z) \cos(\omega_2 t + k_2 z) ] \end{aligned} \quad (6)$$

From eq. 6 it can be seen that the first order nonlinear polarization contains components with various combination frequencies:

$$P_{2\omega_1} = 2d \epsilon_0 \epsilon_1^2 \cos 2(\omega_1 t + k_1 z) \quad (7)$$

$$P_{2\omega_2} = 2d \epsilon_0 \epsilon_2^2 \cos 2(\omega_2 t + k_2 z) \quad (8)$$

$$P_{\omega_1+\omega_2} = 2d \epsilon_0 \epsilon_1 \epsilon_2 \cos\{(\omega_1 + \omega_2)t + (k_1 + k_2)z\} \quad (9)$$

$$P_{\omega_1-\omega_2} = 2d \epsilon_0 \epsilon_1 \epsilon_2 \cos\{(\omega_1 - \omega_2)t + (k_1 - k_2)z\} \quad (10)$$

The second harmonics of both waves, as well as sum and difference frequency terms result along with a DC term as well.

From eq. 2 it is clear that:

$$-P_{\text{total}} = \epsilon_0 (-\chi^{(1)}E - \chi^{(2)}EE - \chi^{(3)}EEE - \chi^{(4)}EEEE - \dots) \quad (11)$$

The symmetry operator  $I_{\text{op}}$  gives:  $I_{\text{op}}P = -P$  and  $I_{\text{op}}E = -E$  and applying it eq. 2 gives:

$$I_{\text{op}}P_{\text{total}} = -P = \epsilon_0 (-\chi^{(1)}E + \chi^{(2)}EE - \chi^{(3)}EEE + \chi^{(4)}EEEE + \dots) \quad (12)$$

Comparing eq.11 with eq.12 shows that consistency only exists for  $\chi^{(2)}EE = -\chi^{(2)}EE$ , hence,  $\chi^{(2)}$  must be zero. Thus, in all media with inversion symmetry have  $\chi^{(2)} = 0$ . So in order to realize the  $\chi^{(2)}$  effects, the crystal must have to be noncentrosymmetric.

The nonlinear susceptibility is defined to be  $\chi^{(2)} = 2d_{ijk}$ . The susceptibility  $\chi_{ijk}$  and nonlinear coefficient  $d_{ijk}$  are tensors; the index  $i$  can have the values 1,2 or 3 corresponding the respective crystal axes  $x$ ,  $y$  or  $z$  and  $jk$  can have the values  $jk = 1; 2; 3; 4; 5$  or  $6$  corresponding to the combinations of axes  $xx$ ,  $xy = yx$ ,  $xz = zx$ ,  $yy$ ,  $yz = zy$  and  $zz$ . For instance, for the term  $d_{31}$  the polarization of the pump wave is along the  $z$ -axis, the polarizations of the generated waves are along the  $x$ -axis.

## Anharmonic Oscillator:

The equation of motion for an anharmonic oscillator can be written as,

$$d^2r/dt^2 + 2\gamma dr/dt + \omega_0^2 r - \xi r^2 = - (e/m)E \quad (13)$$

Equation 13 does not have a simple exact solution because of the anharmonic term ( $\xi r^2$ ). The anharmonic contribution is usually small, so a solution in the form of a power series:

$$r_j = a_j E^j \quad (14)$$

where  $j$  is 1,2,3,4,..... can be tried. Substituting in eq. 13 and collecting terms of same order,

$$d^2r_1/dt^2 + 2\gamma dr_1/dt + \omega_0^2 r_1 = - (e/m)E \quad (15)$$

$$d^2r_2/dt^2 + 2\gamma dr_2/dt + \omega_0^2 r_2 = \xi r_1^2 \quad (16)$$

From eq. 16, it follows that the nonlinearity is  $r_2 = a_2 E^2$ , which corresponds to the first nonlinear term in the polarization (eq. 2). When higher-order terms of  $r$  are also taken into account, it is found that they contribute to higher-order nonlinearities.

## Anisotropy:

The natural frequency  $\omega_0$  and the refractive index of a material are influenced by the interaction between the atoms constituting the medium. For isotropic medium an applied electric field  $E_x$  generates a dielectric displacement  $D_x$  lying only along x direction i.e.  $D_y = 0 = D_z$ . The dielectric constant  $D$  in anisotropic materials is a second-rank tensor i.e. in such a medium  $E_x$  will in general generate a dielectric displacement having all three components.

$$D_x = \epsilon_{xx}E_x \quad D_y = \epsilon_{yx}E_x \quad D_z = \epsilon_{zx}E_x \quad (17)$$

And thus  $\epsilon$ , the dielectric permittivity of the medium, is now a tensor. It can be shown that  $\epsilon_{kl}$  (where both  $k$  &  $l$  run over  $x, y, z$ ) is a symmetric tensor with 6 ( $\epsilon_{xx}, \epsilon_{yy}, \epsilon_{zz}, \epsilon_{yz}, \epsilon_{xz}, \epsilon_{xy}$ ) independent components. Considering principal dielectric axes,

$$\begin{pmatrix} D_x \\ D_y \\ D_z \end{pmatrix} = \begin{pmatrix} \epsilon_x & 0 & 0 \\ 0 & \epsilon_y & 0 \\ 0 & 0 & \epsilon_z \end{pmatrix} \begin{pmatrix} E_x \\ E_y \\ E_z \end{pmatrix}$$

$\epsilon_x, \epsilon_y, \epsilon_z$  are principal dielectric permittivities.

$$\epsilon_x = \epsilon_y = \epsilon_z \Rightarrow \text{Isotropic} ; \quad \epsilon_x = \epsilon_y \neq \epsilon_z \Rightarrow \text{Uniaxial} ; \quad \epsilon_x \neq \epsilon_y \neq \epsilon_z \Rightarrow \text{Biaxial}$$

And finally,  $(\epsilon/\epsilon_0)^{1/2} = [1 + \chi^{(1)}]^{1/2} = n$  (**refractive index**)

## Walk-off or Double Refraction:

In birefringent media, the direction of wave propagation (direction of  $\mathbf{k}$ ) for an extraordinary ('e') wave is seen to "walk-off" the axis of the ordinary ('o') beam (fig.1).

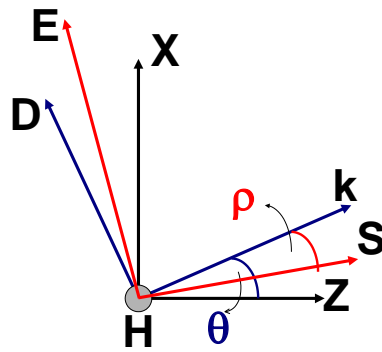


**Fig. 1.** The angle ( $\rho$ ) between  $\mathbf{k}$  and  $\mathbf{S}$ .  $\mathbf{H}$  is perpendicular to the figure.

From Maxwell's Equations,

$$\vec{\nabla} \times \vec{E} = i(\vec{E} \times \vec{k}) = -i\omega\mu_0\vec{H}$$

$$\vec{\nabla} \times \vec{H} = i(\vec{H} \times \vec{k}) = i\omega\vec{D}$$

$$\vec{E} \times \vec{H} = \vec{S}$$

(18 a,b,c)

We have considered the transmission of a monochromatic plane wave through an anisotropic crystal and the traveling wave has the  $e^{i(\omega t - kz)}$  dependence. For such wave we can replace the operator  $\nabla$  by  $(-ik)$  and  $\partial/\partial t$  by  $i\omega$ . From eq. 18(a),  $\mathbf{H}$  is perpendicular to  $\mathbf{E}$  and  $\mathbf{k}$ , while from eq. 18(b),  $\mathbf{D}$  is perpendicular to  $\mathbf{H}$  and



**k**. Thus **D**, **k**, **E** and **S** [from eq. 18(c)], are all in a plane perpendicular to **H**. The angle between **k** and **S** is called walk-off angle  $\rho$  and for uniaxial crystal for wave vector propagation in xz plane at an angle  $\theta$  with respect to the optic axis (z direction in fig. 1) can be expressed as:

$$\tan \rho = \frac{1}{2} n_e^2(\theta) \left( \frac{1}{n_e^2} - \frac{1}{n_o^2} \right) \sin 2\theta \quad (19)$$

For noncritical angle i.e. when  $\theta = 90^\circ$ ,  $\rho$  becomes zero. For a beam of constant radius  $w$ , 'o' and 'e' beams become physically separated in a distance,

$$L_\rho = 2w/\tan\rho \approx 2w/\rho \quad (20)$$

As an example, for a beam diameter of 1 mm and  $\rho = 2^\circ$ , this distance is approximately 3 cm. Beams that do not physically overlap cannot interact. So the walk-off effect is a serious detriment to frequency conversion efficiency.

### Symmetry Considerations for $\chi^{(2)}$ :

It can be seen that  $\chi_{ijk}$  will have 81 different independent components. Fortunately there are two important symmetry conditions that help to reduce the number considerably.

#### A. Overall Permutation Symmetry:

$$\begin{aligned} \chi_{ijk}(\omega_1, -\omega_2, \omega_3) \\ &= \chi_{jki}(-\omega_2, \omega_3, \omega_1) \\ &= \chi_{kij}(\omega_3, \omega_1, -\omega_2) \end{aligned} \quad (21)$$

The frequencies may be freely permuted, provided the Cartesian indices  $i$ ,  $j$  and  $k$  are permuted with the frequencies. This reduces the number of components to 27 from 81.

#### B. Kleinman's Conjecture:

$$\chi_{ijk} = \chi_{jki} = \chi_{kij} \quad (22)$$

This last symmetry condition is valid only when all the three interacting frequencies are within the transmission region (without any cut-off) of the nonlinear medium being considered.

### Coupled Amplitude Equations:

Considering:

1.  $E_i(z,t) = E_i(z) \exp[-i(\omega_i t - k_i z)] + \text{c.c.}$
2.  $P_1(z,t) = 2\varepsilon_0 d E_2^*(z) E_3(z) \cdot \exp[-i\{(\omega_3 - \omega_2)t - (k_3 - k_2)z\}]$
3.  $\mathbf{D} = \varepsilon_0 [1 + \chi^{(1)}] \mathbf{E} = \varepsilon \mathbf{E} + \mathbf{P}_{NL}$
4.  $\mu = \mu_0$  (nonmagnetic) &  $\sigma = 0$  (charge-free)

$$5. \nabla^2 E_i - \mu \epsilon_0 \partial^2 E_i / \partial t^2 = \mu_0 \partial^2 P_{NL} / \partial t^2$$

6. SLOWLY-VARYING AMPLITUDE APPROXIMATION:

The distance over which  $dE/dz$  changes appreciably is large compared to the wavelength so that,

$$dE/dz \gg d^2E/dz^2$$

One gets,

$$\begin{aligned} \frac{dE_1(z)}{dz} &= i \frac{\omega_1^2 d}{c^2 k_1} E_2^*(z) E_3(z) e^{i(k_3 - k_2 - k_1)z} \\ \frac{dE_2(z)}{dz} &= i \frac{\omega_2^2 d}{c^2 k_2} E_1^*(z) E_3(z) e^{i(k_3 - k_2 - k_1)z} \\ \frac{dE_3(z)}{dz} &= i \frac{\omega_3^2 d}{c^2 k_3} E_1(z) E_2(z) e^{-i(k_3 - k_2 - k_1)z} \end{aligned} \quad 23 \text{ (a,b,c)}$$

These are the three coupled amplitude equations showing mutual dependency of power between the interacting frequencies. For small signal approximations i.e. when there is no pump depletion then,

$$E_3 = i \frac{\omega_3^2 d}{c^2 k_3} E_1 E_2 \int_0^L e^{i\Delta k z} \quad (24)$$

$$\& \sin ce \quad (25)$$

$$\frac{P_i}{A} = \frac{1}{2} E_i E_i^* \sqrt{\frac{\epsilon_i}{\mu_0}} = \frac{1}{2} n_i c \epsilon_0 E_i E_i^*$$

One obtains the following expression for the intensity of the generated frequency as,

$$\frac{P_3}{A_3} = \frac{2 \omega_3^2 d^2 L^2}{n_1 n_2 n_3 c^3 \epsilon_0} \frac{P_1 P_2}{A_1 A_2} \left[ \frac{\sin\left(\frac{\Delta k L}{2}\right)}{\left(\frac{\Delta k L}{2}\right)} \right]^2 \quad (26)$$

Where  $P_1$  and  $P_2$  are the power of the input frequencies  $\omega_1$  and  $\omega_2$ ;  $A_1$  and  $A_2$  are the area of the input beams;  $n_i$ 's are refractive indices of  $\omega_i$ 's;  $L$  is the crystal length and  $\Delta k$  is the phase-mismatch parameter. The above eq. (26) clearly shows the dependence of intensity ( $I_3 = P_3/A_3$ ) of the generated radiation on different parameters of the nonlinear crystal, like its nonlinear coefficient, length, refractive indices etc. It also shows that  $I_3$  is proportional to the product of the intensities ( $I_1$  and  $I_2$ ) of the parent input beams.

### Manley-Rowe Relations:

From the coupled amplitude equations 23 (a,b,c) given above, multiplying both sides by  $\epsilon_0 E_i^*(z)/2$ ,

$$(\frac{1}{2}\omega_i)\epsilon_0 n_i c E_i^*(z) [dE_i(z)/dz] = (\epsilon_0 i d/2) E_i^*(z) E_j^*(z) E_k(z)$$

& remembering,

$$d(E_i E_i^*)/dz = (2/\epsilon_0 n_i c) [d(P_i/A_i)/dz]$$

One gets,

$$\frac{1}{\omega_1} \frac{d}{dz} \left( \frac{P_1}{A_1} \right) = \frac{1}{\omega_2} \frac{d}{dz} \left( \frac{P_2}{A_2} \right) = -\frac{1}{\omega_3} \frac{d}{dz} \left( \frac{P_3}{A_3} \right) \quad (27)$$

i.e.

$$\begin{aligned}
 & (\text{Change in intensity at } \omega_1)/\omega_1 \\
 &= (\text{Change in intensity at } \omega_2)/\omega_2 \\
 &= -(\text{Change in intensity at } \omega_3)/\omega_3
 \end{aligned}
 \tag{28}$$

This is the famous Manley-Rowe relation. The ‘-’ sign in the last one is very important.

**Consequences:**

For SFM [ $\omega_3 = \omega_1 + \omega_2$ ] both lasers ( $\omega_1$  &  $\omega_2$ ) will loose power which is gained by the generated beam ( $\omega_3$ ).

For DFM [ $\omega_1 = \omega_3 - \omega_2$ ] source laser at  $\omega_3$  will loose power not only to the generated beam ( $\omega_1$ ) but also to the other source ( $\omega_2$ ). This is the significance of the ‘-’ sign in last one.

**Phase-Matching:**

It refers to the tendency, when propagating through a nonlinear medium, of the generated wave to become out of phase with the induced polarization after some distance. It involves precise control of the indices of the three frequencies involved in the mixing process to match the velocities of propagation of the polarization waves and the electromagnetic wave which they generate. It can be seen that the generated signal is  $90^\circ$  out of phase with the polarization wave when  $\Delta k = 0$ . It can be shown that this makes it possible to couple the energy from the polarization wave into the generated wave. But for  $\Delta k \neq 0$  this favorable condition exists only at  $L = 0$  and after one coherence length ( $L_c = \pi/\Delta k$ ) the phase of the signal will change exactly by  $90^\circ$ . Thus power flow changes sign. So if  $L = 2L_c$  no generation will occur.

One of the most important ways to achieve phase-matching is to compensate the dispersion of the nonlinear crystal by its birefringence. And too small birefringence will not be able to make such compensation as shown in fig. 2 and hence will not allow this angle phase-matching.

**Birefringence – Phase Matching**

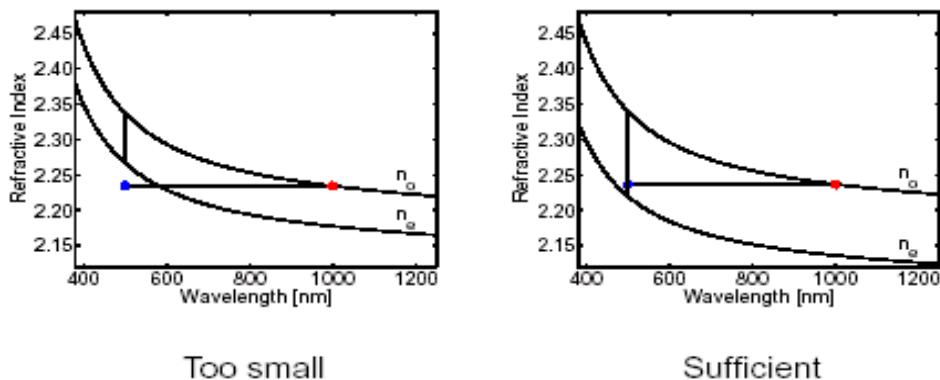


**Fig. 2** The nonlinear crystal must have adequate birefringence to compensate its dispersion.

In fig. 3 below it can be seen that in the given negative uniaxial nonlinear medium one can achieve the SHG of 1064 nm radiation, by equating the phase-velocities of ‘o’ polarized 1064 nm beam and that of the

'e' polarized 532 nm beam by rotation of wave propagation angle  $\theta$  which the interacting beams make with the crystal optic axis inside the crystal. And since,

$$\begin{aligned} n^{\text{ord}} &= n_o \\ n^{\text{ext}} = n^e(\theta) &= \left[ \frac{\cos^2 \theta}{n_o^2} + \frac{\sin^2 \theta}{n_e^2} \right]^{-1/2} \end{aligned} \quad 29(a,b)$$

hence the phase-matching (PM) condition for above interaction will be,

$$n_1^o = n_2^e(\theta) \quad (30)$$

However if the condition be such that  $n_1^o = n_2^e$  then the phase-matching angle  $\theta$  will be  $90^\circ$  as is the case shown for second harmonic generation of 532 nm in Fig. 3. In such case the interaction is said to be non-critically phase-matched. SHG of 532 nm is obviously fourth harmonic of 1064 nm and hence it is denoted as FHG in the figure.

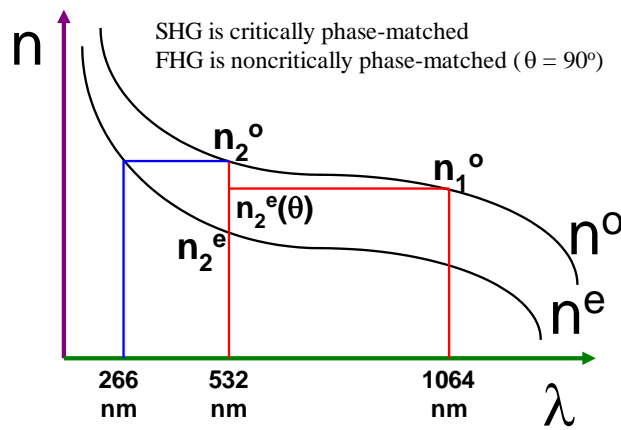


Fig. 3. Angle phase matching for SHG.

#### PM Conditions for negative uniaxial crystals:

For sum frequency generation SFG:  $(1/\lambda_1 + 1/\lambda_2 = 1/\lambda_3) \quad \lambda_1 > \lambda_2 > \lambda_3$

Type-I	Type-IIA	Type-IIB	
ooe	eoe	oee	(31a,b,c)

For difference frequency generation DFG:  $(1/\lambda_1 - 1/\lambda_2 = 1/\lambda_3) \quad \lambda_1 < \lambda_2 < \lambda_3$

Type-I	Type-IIA	Type-IIB	
eoo	eoe	eoo	(32a,b,c)

For positive uniaxial crystal the conditions can be obtained simply by changing the ordinary polarization by extraordinary and vice-versa. For example, for SFG, the conditions will be eeo, oeo and eoo respectively for Type-I, Type-IIA and Type-IIB.

#### Critical issues of Material Selection:

1. Nonlinear coefficient must be high.
2. Higher damage threshold is always an important advantage for improving conversion efficiency.

3. The crystal should have enough birefringence to allow phase-matching for different interactions.
4. The crystal should have large transparency range.
5. The crystal length is an important parameter as the conversion efficiency increases by  $L^2$ . So it is important that the crystal can be available in large size.
6. Stability is very important since if the crystal is hygroscopic then its polished surfaces will easily become opaque and thus it cannot be used. Of course thermal ovens can be used to tackle such problems, but it will mean additional cost and extra care.
7. Optical homogeneity of the crystal is very essential for getting high conversion efficiency.

For example, detailed characteristics of some important UV-VIS-NIR and IR nonlinear crystals are respectively given in Table-1 and Table-2.

### Assessments of Nonlinear Materials:

S. K. Kurtz's powder method, demonstrated in 1968, represents the first real means of screening, experimentally, large numbers of unknown materials for nonlinear activity, without having to perform the slow and expensive task of growing good quality crystals of each material. Kurtz showed that it is possible by measurements on powders, to ascertain whether a crystal has large or small nonlinearity and whether it can be phase-matched.

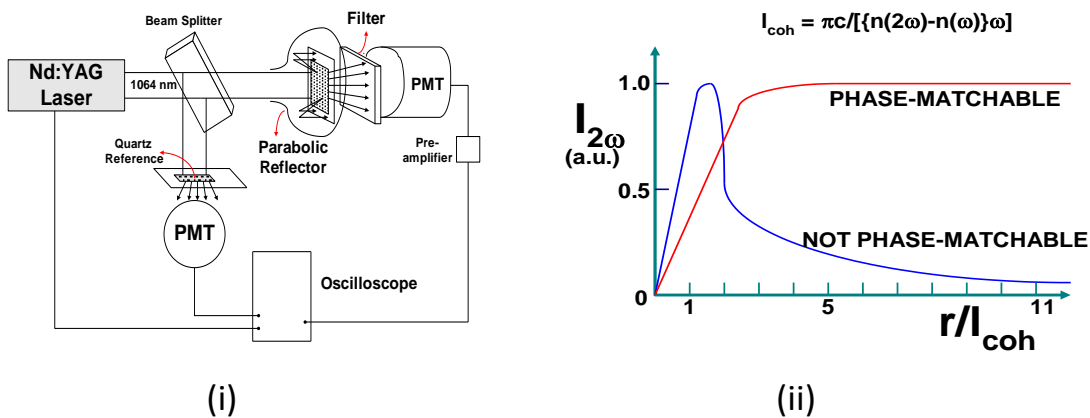


Fig. 4. (i) Schematic set up of Kurtz powder method and (ii) the typical response of SHG with particle size of powders of phase-matchable and non-phase-matchable crystals.

In brief, in the experiment the sample is first grinded such that one can obtain several powdered forms. While each powder consists of a uniform particle size, but particle sizes are in increasing order of magnitude in different powders. Each powdered sample is taken on a glass slide and positioned as shown in the figure inside the chamber having parabolic reflector. For each sample, the SHG will increase till  $r/L_c = 1$  where  $r$  is the radius of the particle in the sample being examined. However, when  $r > L_c$ , if the crystal is not phase-matchable, then the SHG starts to decrease. However, if the crystal is phase-matchable then, the generation will ultimately saturate as an increase in  $r$  will decrease the number of particles in the fixed place. In this way using only powdered form of a sample, one can easily ascertain whether the crystal is suitable for nonlinear frequency conversion devices or not.

**Table-1. Characteristics of some UV-VIS-NIR crystals:**

Crystal (Point Group)	Transmission ( $\mu\text{m}$ )	Birefringence	Nonlinearity $d \times 10^{-12}$ (M/V)	Surface Damage Threshold ( $\text{MW}/\text{cm}^2$ )
KDP [ $\bar{4}2m$ ]	0.2–1.55	– 0.04	0.38	1000
DKDP [ $\bar{4}2m$ ]	0.2–2.15	– 0.04	0.38	1000
BBO (3m)	0.189 – 3.5	– 0.11	2.2	13500
LBO (mm2)	0.16 – 2.6	– 0.05	1.4	27000
CLBO [ $\bar{4}2m$ ]	0.18 – 2.75	– 0.47	1.0	29000
LB <sub>4</sub> (4mm)	0.16 – 3.5	– 0.055	0.15	40000
KTP (mm2)	0.35 – 4.5	+ 0.09	3	500
KTA (mm2)	0.35 – 5.2	+ 0.08	3	500
LiNbO <sub>3</sub> (3m)	0.33 – 5.5	– 0.08	4.7	50
LiIO <sub>3</sub> (6)	0.3 – 6.0	– 0.14	4.1	125

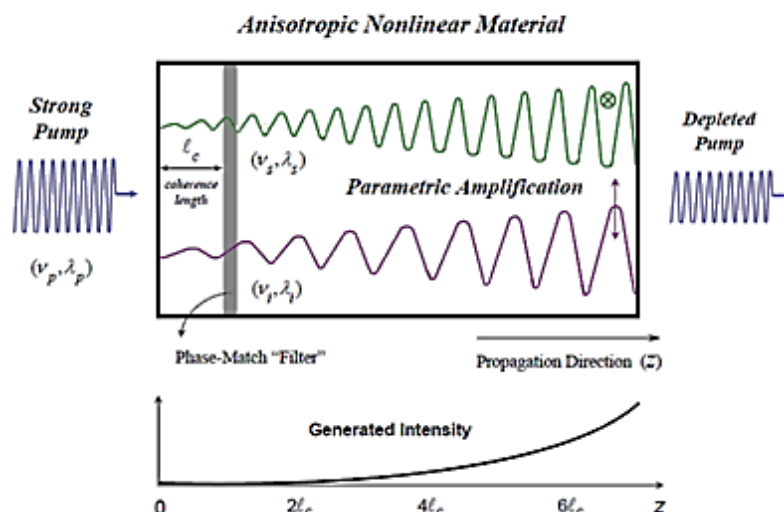
**Table-2. Characteristics of some IR crystals:**

Material	AgGaS <sub>2</sub>	AgGaSe <sub>2</sub>	ZnGeP <sub>2</sub>	GaSe	CdGeAs <sub>2</sub>	HgGa <sub>2</sub> S <sub>4</sub>	AgGa <sub>x</sub> In <sub>1-x</sub> Se <sub>2</sub>	Tl <sub>3</sub> AsSe <sub>3</sub>
d coeff. (pm/V)	12	33	75	54	236	35	36 (x = 0.58)	20
Transparency ( $\mu\text{m}$ )	0.50 – 13.2	0.76 – 18.0	0.72 – 12.3	0.65 – 18.0	2.60 – 17.8	0.50 – 14.3	0.8 – 18.0	1.3 0 – 17.0
Birefringence	– 0.053	– 0.033	+ 0.039	– 0.373	+ 0.096	– 0.04	– 0.018	– 0.18
dB/dT X 10 <sup>-5</sup>	0.178	0.26	1.3	15.0	0.23	–	–	8.4
Thermal Conductivity (W/cmK)	0.015	0.011	0.36	0.162	0.042	0.039	0.011	0.0035
Laser Damage Threshold	0.25 J/cm <sup>2</sup>	0.5–3 J/cm <sup>2</sup>	3–10 J/cm <sup>2</sup>	3 J/cm <sup>2</sup>	20–40 MW/cm <sup>2</sup>	60 MW/cm <sup>2</sup>	40 MW/cm <sup>2</sup>	35 MW/cm <sup>2</sup>
Shortest Pump $\lambda$	0.6 $\mu\text{m}$	1.27 $\mu\text{m}$	1.7 $\mu\text{m}$	0.7 $\mu\text{m}$	2.7 $\mu\text{m}$	0.5 $\mu\text{m}$	1.27 $\mu\text{m}$	1.35 $\mu\text{m}$

# Optical Parametric Oscillator:

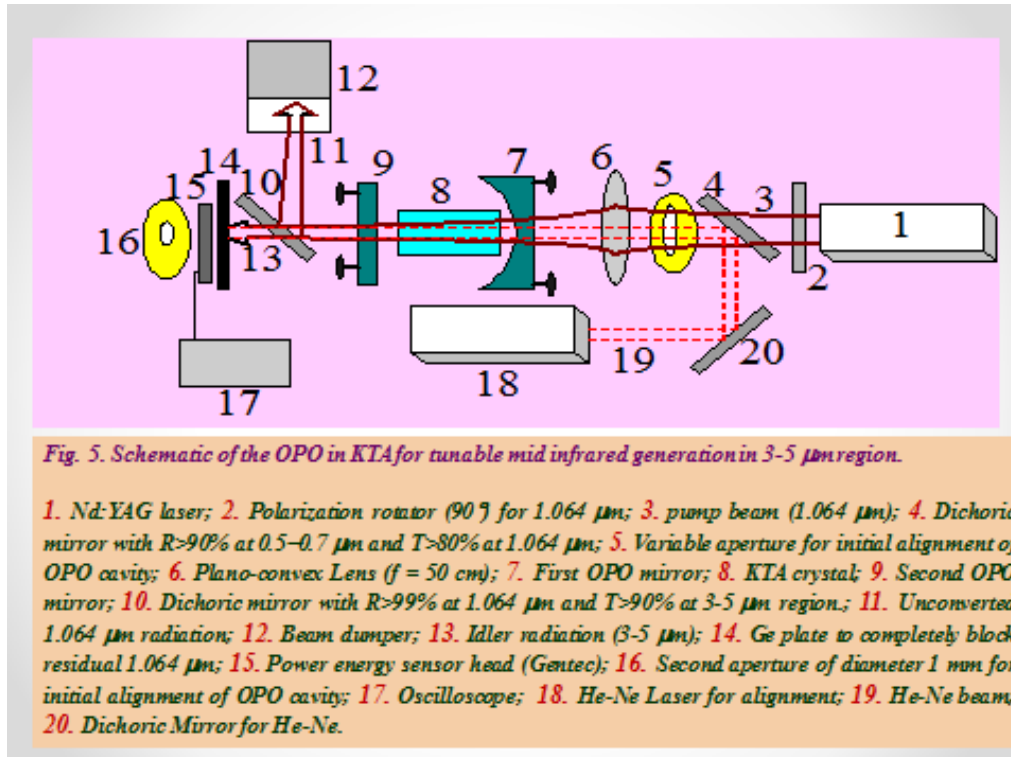
LASER	OPO
1. Needs population inversion	1. No population inversion is needed. The Signal and idler are amplified at the expense of the energy of the pump wave instead of energy stored in the form of molecular excitation in the nonlinear medium.
2. Active medium needed	2. Nonlinear crystal
3. Threshold condition	3. Threshold condition exists for pump intensity.
4. Initial photon comes from spontaneous emission	4. Initial photon triggering OPO comes from parametric fluorescence.
5. Tuning range is quite low.	5. Tuning range is quite high.
6. Laser can be operated with spatially incoherent pump sources.	6. It requires relatively high optical intensity and high spatial coherence of its pump. In most cases a laser is used to pump an OPO.
7. Thermal lensing needs special attention.	7. As OPOs are mostly operated with all wavelengths involved lying well within the transparency region, there is normally no such thermal lensing.

## Phase-Matching



The initial photon in case of OPO comes from parametric fluorescence. *In this process no molecule drops from an excited energy level to a lower one with the emission of a photon.* In parametric fluorescence a molecule exposed to a radiation of frequency  $\omega_1$  can emit two photons at  $\omega_2$  and  $\omega_3$  such that  $\omega_1 = \omega_2 + \omega_3$ . In this process the internal state of the molecule remains same before and after the emission of the two photons. The molecule has very loosely speaking acted to split the incident photon into two outgoing photons.

The main attraction of OPO is that the signal and idler wavelengths, which are determined by a phase-matching condition, can be varied in wide ranges. Thus it is possible to access wavelengths (e.g. in the mid-infrared, far infrared or the THz spectral region) which are difficult or impossible to obtain from any laser and wide wavelength tunability is also possible.



The input mirror of the OPO (where the pump beam is coupled into the resonator) should have high transmission at the pump wavelength. The output mirror could transmit the pump light or reflect it. The two alternatives are referred to as single-pass pump and double-pass pump, respectively. The latter approach has potential for higher conversion efficiency, but an optical isolator is normally required between the pump source and the OPO to prevent undepleted pump light to interfere with and potentially harm the pump source. The OPO intracavity fluence will be higher with such geometry, increasing the risk for optical damage.

### An Interesting Result:

Crystal: GaSe ( $\theta = 0^\circ$  cut & L = 2 cm)

$\lambda_1 = 1.064 \mu\text{m}$ ;  $I_1 = 17 \text{ MW/cm}^2$

$\lambda_2 = 1.094 - 1.76 \mu\text{m}$  (OPO);  $E_2 = 5 \text{ mJ}$  (max)

Pulse Width ~ 5 ns.

$\lambda_3 = 2.7 - 38.4 \mu\text{m}$

Reference: W. Shi & Y. J. Ding, Appl. Phys. Lett. 84 1635 (2004)

### Some Reference Books:

1. *Applied Nonlinear Optics*, F Zernick and J E Midwinter, Dover Publications Inc.
2. *Principles of Nonlinear Optics*, Y R Shen, Wiley-Interscience.
3. *Handbook of Nonlinear Optics*, R L Sutherland, CRC Press.
4. *Handbook of Nonlinear Optical Crystals*, V G Dmitriev, G G Gurzadyan and D N Nikogosyan, Springer.